

# **Synthesis of CuZn MOF MXene composite for application as an antibacterial coating on contact lens**

Master's thesis

MDP in Physical and Chemical Sciences

30<sup>th</sup> May 2025

Author:

Misbah Saleem

Supervisor:

Prof. Carita Kvarnström

Prof. Hongbo Zhnag

University of Turku

Department of Chemistry

## Abstract

The benefits and convenience of contact lenses are accompanied by few complications. Contact Lens Complications (CLC) includes microbial keratitis, blepharitis, fungal infections, acanthamoeba keratitis, herpes simplex keratitis, herpes zoster keratitis and marginal keratitis. Wearing contact lenses for the extended duration without taking proper cleaning measures, elevate the possibility of bacterial growth on it. The conjunctivitis and keratitis are associated with microbial keratitis caused by certain Gram-positive and Gram-negative bacteria. This research majorly focused on Staphylococcus aureus (S. aureus) and Escherichia coli (E.coli), which are the significant bacteria in originating the eye infection.

This research comprehends on the introduction of CuZn MOF based MXene, on contact lenses to prevent bacterial growth.  $Ti_3C_2T_x$  MXene was coupled with methyl imidazole based CuZn MOF, as the MOF derived composites exhibits high antibacterial activity (Mofei Shen, 2020). MOF were prepared using Zinc(II) nitrate hexahydrate, Copper(II) nitrate trihydrate, methylimidazole and methanol. These MOF composites were than combined and analyzed with four different concentrations (1mg/ml, 500 $\mu$ g/ml, 250 $\mu$ g/ml 125 $\mu$ g/ml and 62.5 $\mu$ g/ml) of MXene using magnetic stirrer for overnight. The CuZn-MXene composite was later analyzed using SEM, TEM, FTIR and XRD. The antibacterial activity of this MXene composite was tested on E.coli and S. aureus bacteria by colonies growth on nutritive agar plates. Subsequently, the contact lens were also prepared by combining cross linker polymer, lithium phenyl 2,4,6 trimethyl benzoyl phosphate (LAP), merged with hyaluronic acid methacrylate (HAMA) and deionized water.

**Keywords:** MXene, metal organic framework, CuZn, contact lens, ocular diseases

## Contents

Abstract	
1. Introduction to MXene	1
1.1 MAX Phase	3
1.2 Fabrication of MXene	4
1.3 Delamination Process	5
1.4 Applications of MXene	6
2. Introduction to MOF	8
2.1 MOFs and their antibacterial behavior	8
2.2 Manufacturing of MOFs	9
2.3 Examples of MOF and their applications	11
2.4 Classification of MOF	12
3. Introduction to contact lenses	12
3.1 Properties and Manufacturing of CL	14
4. Drug delivery Mechanism	15
5. Antimicrobial Resistance (AMR)	17
5.1 Gram positive and Gram negative bacteria	17
6. Composites used for antimicrobial purposes	19
7. Materials and Methods	24
7.1 Materials	24
7.2 Characterization studies	24
7.4 Preparation of MXene and CuZn MXene composite	24
7.5 Preparation of bacterial culture	25
7.6 Negative Results	27
8. Results	28
8.1 X-Ray Diffraction (XRD) analysis	28
8.2 Fourier Transform Infrared (FTIR) analysis	29
8.3 Scanning Electron Microscopy (SEM) imaging	30
8.4 Transmission Electron Microscopy (TEM) imaging	31
8.5 Antibacterial Analysis	31
9. Contact Lens formation	32
10. Discussion and Conclusion	32
11. Future aspects	33
References	33

## **Acknowledgment**

I would like to extend my gratitude to my supervisor Prof. Carita Kvarnstrom for her unwavering support throughout my thesis project. I convey my appreciation to Prof. Hongbo Zhang also for allowing me to conduct experiments for the project and providing with resources and support. Lastly, profound gratitude to all the professors for their participation in the experimental studies of this project my thesis owes its completion to their invaluable contributions.

## Abbreviations

TMDs	transition metal dichalcogenides
DMSO	Dimethyl sulfoxide
CXL	Collagen Cross-Linking
pHEMA	poly(2-hydroxyethyl methacrylate)
AgNPs	Silver nanoparticles
ROS	Reactive Oxygen Species
PEI	polyethylenimine
PDMAEMA	poly(2-(dimethylamino)ethyl methacrylate)
LiF	lithium fluoride
DI	deionized water
SEM	Scanning Electron Microscopy
LB	Luria-Bertani
PBS	Phosphate Buffer Solution
XRD	X-Ray Diffraction
LAP	Lithium phenyl 2,4,6 trimethyl benzoyl phosphate
HAMA	hyaluronic acid methacrylate
PDT	Photodynamic Therapy
AMR	Antimicrobial Resistance
MI	Molecular imprinting
LAG	Liquid Assisted Grinding
BTC	Benzenetricarboxylic
PCN	Porous coordination networks
CLC	Contact less complications

## **Preface**

The increased number of bacterial infections especially in the field of ocular diseases leads to develop advance bactericidal agents to repress this issue and enhance the eye protection. Conventional antimicrobial agents have shown restrictions concerning biocompatibility, cell inhibition, transparency and potent for long term. In this research work, fusion of MXene with metal organic frameworks manifested synergistic out-turn owing to their physical, chemical and antimicrobial characteristics. There were numerous materials developed for this purpose such as silver nanoparticles (excellent antimicrobial activity but have issues of cytotoxicity and eye irritation), ammonium compounds (not only kill bacteria but also potent for causing dermatitis and strong rashes) and peptides (biocompatible but costly). Graphene also successfully experimented as antimicrobial agent but failed in durability. MOFs shows good antibacterial activity due to charged metals yet ineffective in controlled drug release. By virtue of these issues there is a necessity of developing a material which overcome aforementioned complications. This research inspects the synthesis of CuZn MOF MXene composite attributed to its properties such as wide-ranging antimicrobial effect from copper and zinc ions, mechanical strength inclusive of hydrophilicity and conductivity provided by MXene. The porous structure of metal organic framework benefits in terms of controlled and efficient drug release. This work aims to bestow in developing advanced materials by merging MOFs and MXene.

## **1. Introduction to MXene**

Among 2D materials such as hexagonal boron nitrides, silicene, borophene and phosphorene, in the aspect of field of research, graphene and transition metal dichalcogenides (TMDs) are prominent. Graphene is a monolayer prevalent crystalline carbon allotrope having  $sp^2$  hybridization. Due to graphene's unique physical, chemical and electronic properties, it holds the top position in the list of 2D materials. Properties such as high surface area, of almost  $3000\text{mg}^{-1}$ , 96.6% optical transparency and extraordinary mechanical and chemical strength, due to strong carbon-carbon bonds, makes it suitable for various applications in electronics, catalyst and in the medical field. Graphene can be prepared using top down and bottom up method depending on the desired crystallinity and size of it. Top-down approach (includes mechanical and liquid exfoliation technique) used to obtain single layer graphene while bottom up method (includes chemical vapor deposition and chemical synthesis) is to achieve graphene through self-assembly of small graphene crystals or nanographene. Graphene's sharp edges have benefits in terms of antibacterial activity by disrupting the bacterial cell membrane but challenges of aggregations, degradation over time and limited biocompatibility terminates its usage as antimicrobial agent.

The 2D layered TMDs comprises of stacking of chalcogen atoms with transition metals resulting in a  $\text{MX}_2$  (X-M-X) layered structure, here M consists of transition metals of group IVB –VIII and X is for Sulfur, Selenium and Tellurium from group VIA(1). TMDs are applicable in optoelectronic devices, for instance, photodetectors and light emitting devices. Moreover, they are

also suitable for sensors due to its flexible electronic properties (2). Their consumption as an antibacterial agent is limited owing to the weak dispersion and limited intrinsic activity.

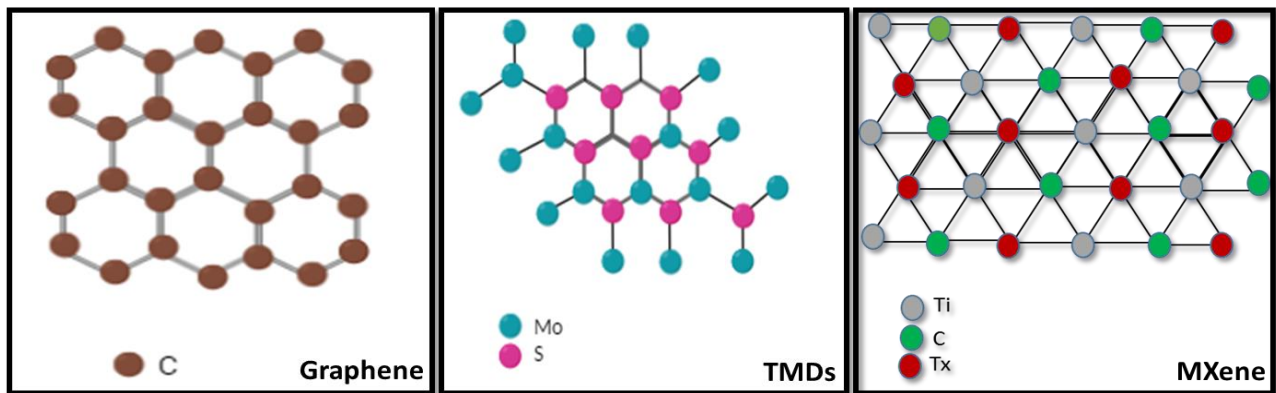


Figure-1 of Graphene, TMDs and MXene.

Along with the discovery of graphene and TMDs, several other 2D layered materials were uncovered and MXenes were amongst them. MXene exhibits layered 2D nanomaterials belongs to transition metal carbide/nitride family.

In the past, Graphene was a leading 2D material for example, graphene oxide has several applications in organic dyes and also holds absorption properties towards metal ions. However, due to the insufficient surface functional groups and having only carbon network makes graphene applications limited. Alternatively, MXene overcome the deficiencies of graphene due to various groups on the layers resulting in chemical and structural stability. MXenes holding transition metal carbides, makes them perfect candidate for electrical conductivity. These 2D materials also hold excellent biocompatibility due to the presence of functional groups which allows to combine with biological molecules maintaining cell proliferation process and biodegradability with minimum cytotoxicity (3,4).

General formula of hexagonal crystal structured MXene is  $M_{n+1}X_nT_x$  where ( $n=1-3$ ) M is a metal from Early Transition metal group such as Ti, V, Mo, Zr etc. X stands for carbon or nitrogen and T denotes the groups present on surface such as -F, -OH, -O- etc. MXenes can be synthesized from

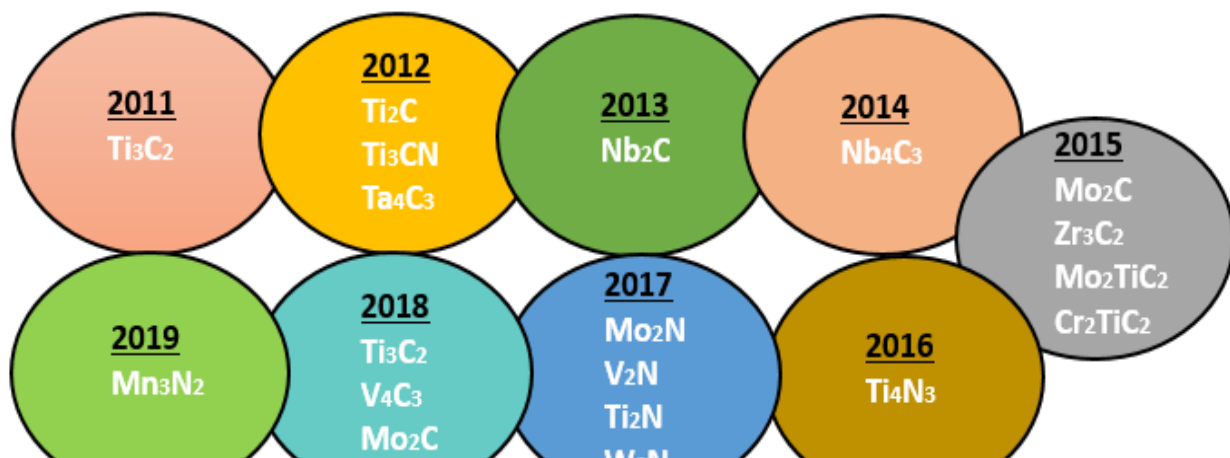


Figure 2- Timeline of MXene synthesis for over the years.

MAX phases, where A can be Zn, Sn, Al and Ga. The MXene used in this project is Titanium based MXene ( $Ti_3C_2T_x$ ) formulated by selective etching of 'A' layers from MAX. The metallic nature of M and covalent nature of X forms strong bonding with each other while the bonding between M and A layers is weak.

In 2011, Material Science professors of Drexel University, Yury Gogotsi and Michel Barsoum, with their group researchers discovered a new member of the 2D transition metal family, MXene (Fei Yu, 2022). Till date composition of 70 types of MAX phases have been formulated and up to 30 MXene are formulated in labs (5). In Fig (2) summary of developed MXene since 2011 are explained. The first discovered MXene was  $M_3X_2T_x$ , for instance,  $Ti_3C_2T_x$ . Other formulated MXene are  $M_2XT_x$  ( $Ti_2CT_x$ ),  $M_4X_3T_x$  ( $Ti_4C_3T_x$ ) and  $M_5X_4T_x$  ( $Mo_4V$ )  $C_4T_x$  (6). MXenes are also available as solid -solutions, discovered in 2012, such as  $Ti_3CNT_x$ ,  $(Ti, Nb)_2CT_x$ , and  $(Cr, V)_3C_2T_x$ . By tuning precursors, new MXenes can be structured for instance high-entropy MXene. Examples of this type of MXene include  $TiVCrMoC_3T_x$  and  $TiVNbMoC_3T_x$  (7).

### 1.1 MAX Phase

The MAX phases are generally composed of an early transition metal (M), elements from group-A (A) and carbon or nitrogen (X) (8).they are present in a hexagonal crystal structure having

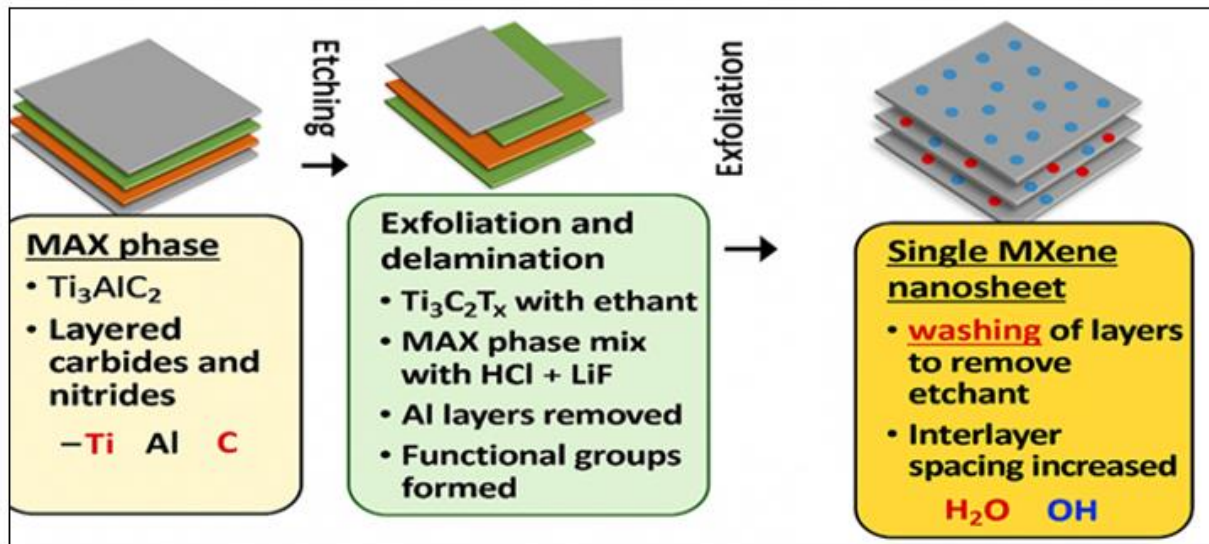


Figure 3- Overview of MXene synthesis.

$M_{n+1}AX_n$  as general formula. Here 'n' represents M layers which separates A layers. The MAX phase is synthesized by providing high temperatures (1300-1600°C) and pressure to heat up the precursors (Ti, Al and C) in compressed and inert environment (9).

### 1.2 The Fabrication of MXene

This process involves the etching of A layers from MAX, as they have relatively weak bonding with M as compared to M-X elements (9) According to the desired MXene specie (10), It can be

synthesized through various etching techniques, for instance, hydrothermal etching, electrochemical etching, molten salt etching and fluoride free and fluoride containing etchant.

### **-Etching by HF**

Initially, despite the corrosive nature of HF, it is used as the etchant to remove the A element from MAX phase. Naguib in 2011 (11), successfully applied 50% HF to MAX phase ( $\text{Ti}_3\text{AlC}_2$ ) to achieve 2D MXene and generating  $\text{AlF}_3$  and  $\text{H}_2$  as byproducts which expelled later resulting in the enlargement of the MXene layers.

### **-Etching with fluoride salt and HCl**

Due to limitations of HF, in 2014 Ghidui (12), used LiF and HCl as an etchant. This complex etchant not only exfoliate the MXene layers but also heads to the enhanced properties of MXene due to presence of cations. Besides, other fluorides such as NaF, KF,  $\text{NH}_4\text{F}$ , etc. can be employed as etchant. Having cations from these mild etchants promotes the additional functional groups on the MXene surface

### **-Hydrothermal Etching**

When temperatures is higher than  $100^\circ\text{C}$  is applied for the exfoliation purposes of MAX, the process is termed as hydrothermal etching. This reaction takes place in an autoclave making it faster and safer. Numerous researches formulated MXene by a hydrothermal etching process. Wang et al. (13), etched A layers from MAX phase using  $\text{NH}_4\text{F}$  as an etchant in autoclave under  $150^\circ\text{C}$  for 24 hours. The hydrothermal conditions, hydrolyzes the  $\text{NH}_4\text{F}$  into  $\text{NH}_3\cdot\text{H}_2\text{O}$  and HF, this HF further reacts with A layers of  $\text{Ti}_3\text{AlC}_2$  to form MXene.

### **-Electrochemical Etching**

This etching procedure expedites the process by providing electric field. This process comprises of anodic and cathodic reactions in the etching solution, here etching solution work as electrolyte. Researchers in 2017, worked on electrochemical etching using  $\text{Ti}_2\text{AlC}$  as electrodes in diluted HCl. This method is not successful for high-volume manufacturing due to layering of carbide derived carbon on unreacted MAX. Molecular intercalation are used to reduce this issue, for instance, tetramethylammonium ion. These intercalated along with etchants react with unetched MAX and enlarge the MXene layer spacing.

### 1.3 Delamination Process

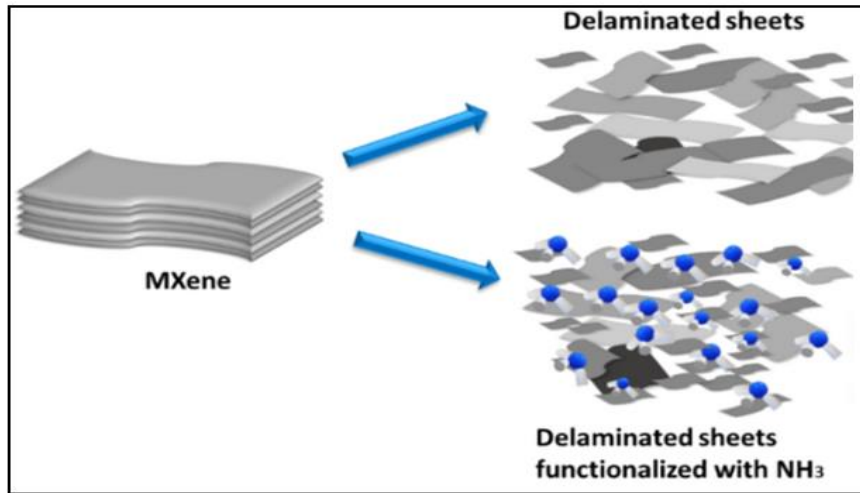


**Figure 4- Delamination process of MXene sheets using intercalant.**(Bidisha Nath, 2023)

After etching the material undergoes a delamination process which is completed in two steps intercalation and sonication, in which spacing between layers gets enlarged using intercalants to yield multi-layer MXene. In the delamination process various functional groups adhere to the layers of MXene acquired from etchants and intercalants (fig. 4). To expand spaces between layers, different ions or organic compounds are incorporated in between layers by using intercalants such as dimethyl sulfoxide, tetrabutylammonium hydroxide and tetramethylammonium hydroxide (14). Sometimes water molecules are also intercalated in between layers from washing process where deionized water is used.

### 1.4 Applications of MXene

#### -Energy Storage

Electrodes in batteries and supercapacitors can be prepared using MXene for charging and storing of energy. Multilayer conductive coatings of MXene are applied on the surfaces of material which even after deformation (i.e. bending and stress) does not change the conductance of that material (15). MXenes have been successfully utilized as anode in Lithium ion batteries (LIBs) in vehicles and electronic devices. Having additional functional groups (F, O, OH etc.), delocalized electrons of transition metals and intercalated ions makes MXene transfer the electrons faster as compare to alone  $Ti_3C_2$  MXene (16). Moreover, studies show that  $Nb_4C_3$  MXene also shows properties suitable for anode material of LIBs. In terms of Non-LIBs (NLIBs), MXene exhibits effective

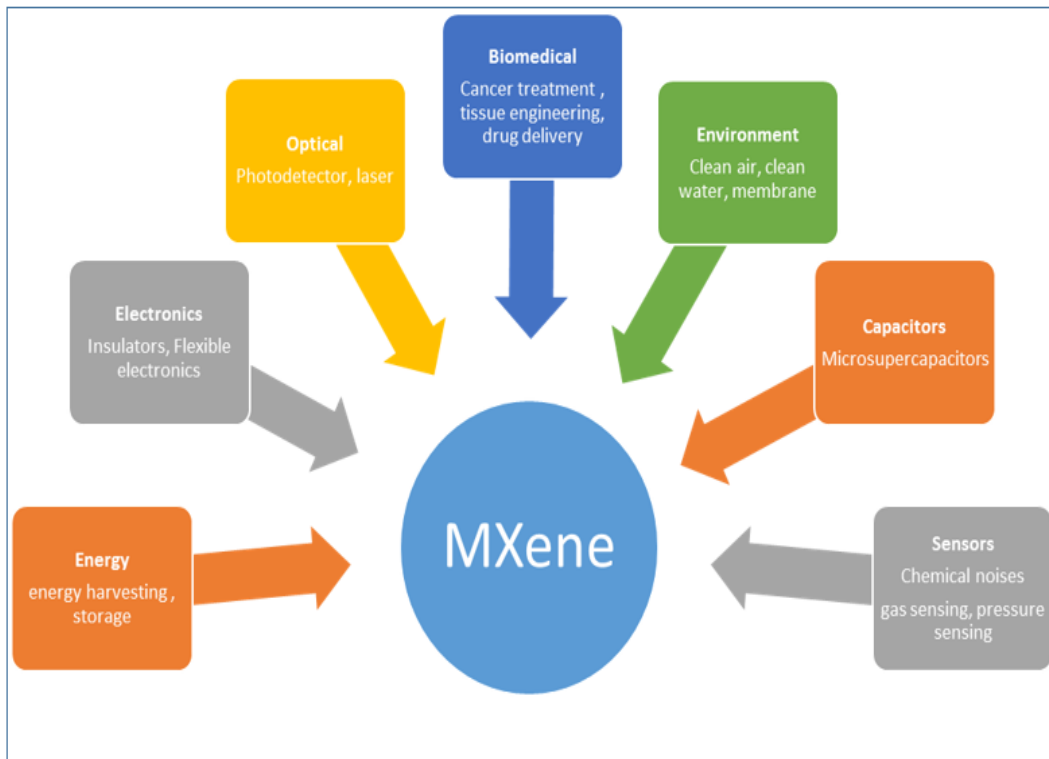


**Figure 5- Applications of MXene**

performance. In NLIBs, MXene is loaded with  $\text{Na}^+$ ,  $\text{K}^+$ ,  $\text{Mg}^+$  and  $\text{Ca}^+$  ion while in LIBs only  $\text{Li}^+$  ions are incorporated between the layers of it (17). Additionally, they can be employed in supercapacitors, due to elevated power densities, as cathode and anode. Recent study proved that hybrid capacitors possess  $\text{Na}^+$  ions with MXene appears to have high performance. Hydrogen storage is another application of MXene in terms of energy storage as it has substantial surface area which provides the storage intermediates.

MXenes have high metallic conductivity especially  $\text{Ti}_3\text{C}_2\text{T}_x$  which is used as supercapacitor (18). Silicon Nano spheres are coupled with MXene sheets, to make Si/MXene composite paper. These papers act as anodes and have greater conductivity in Li-ion batteries than the normal MXene (19).

### **-Sensors**

It has been more than a decade that MXene are applied as sensors (especially biosensors and gas sensors) because of its high surface area, conducting properties and biocompatibility. MXene has been used in biosensors to immobilize hemoglobin for detection of nitrites, as MXene protects the active protein and enables the electron transfer between enzyme and electrode. Because of the porous structure and chemical composition, MXene are used as sensors especially to detect gas (such as ammonia and acetone). The scientists observed that  $\text{NH}_3$  gas is better adsorbed on MXene as compared to other gases ( $\text{H}_2$ ,  $\text{CH}_4$ ,  $\text{CO}$ ,  $\text{N}_2$  and  $\text{O}_2$ ) (20). MXene gas sensors are more efficient than other sensors to detect lethal and toxic gasses (21). MXene based biosensors are also common because of its electrical characteristics.

MXenes are widely used in the biomedical fields due to their mechanical flexibility, hydrophilicity, biocompatibility and light-to-heat conversion capabilities. MXenes are used in making sensors, PTT, drug delivery and many more. Diagnostic imaging is possible because of its intrinsic photothermal performance. Imaging such as MRI (magnetic resonance imaging), PAI (photoacoustic imaging) and luminescence imaging (22). They can be used in limited tissue engineering procedures for instance bones, skin, nerve and heart. MXene exhibits excellent antibacterial and antiviral properties on human immune cells against harmful pathogens owing to its chemical stability, interlayer spacing and many active sites (23).

### **-Desalination of Water**

MXenes can be used in desalination of water and wastewater treatment. For this purpose  $Ti_3C_2$  MXene is used because of their photoactive property. By fusing this MXene with polystyrene we can use it to purify water (24). The properties of MXene, including tunable layers to trap selective ions, the hydrophilic nature, high surface area and photothermal conversion ability makes it an excellent material for rejecting salt molecules (25).

### **-Biomedical Application**

Due to large surface area, MXenes are potential drug carriers for therapeutic procedures, such as, for cancer treatment MXene was loaded with doxorubicin by researchers. The functional groups and the surface morphology collectively showed antibacterial behavior by inhibiting microbial growth. This biocompatibility of MXene makes it easier to be applied in the biomedical devices and wound dressings. MXenes along with hydrogels, are applicable for tissue and bone regeneration (26).

## **2. Introduction to MOF**

In 1965, the research about porous materials attracted other scientists to explore deeper in the field of metal organic frameworks (27). Metal organic frameworks are organic-inorganic hybrid

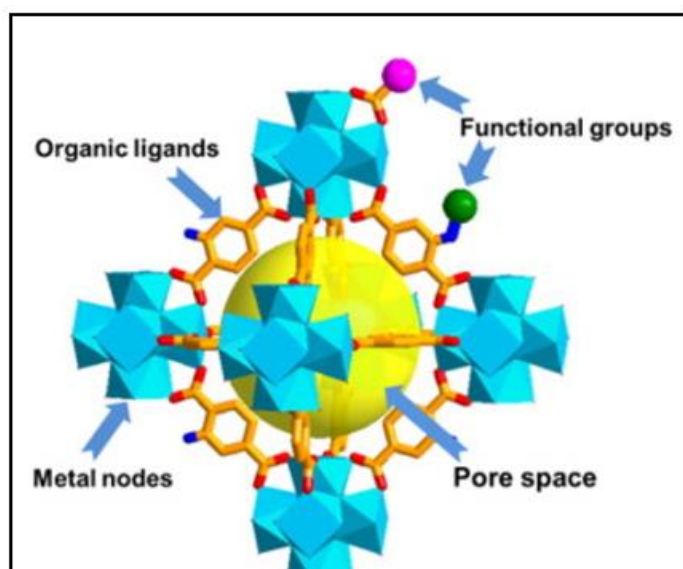


*Figure 6- General structure of MOF (Long Jiao J. Y.-l., 2019)*

compounds, fabricated from inorganic moieties and organic linkers via covalent coordination (fig. 6). The organic linkers are negatively charged molecules consisting of bi- or trivalent carboxylic acids or nitrogen containing aromatics while the inorganic linkers are usually metal ions (metal nodes) and also termed as secondary building units. Due to a linker and nodes structure, MOF forms an ultrahigh porous structure (90% free volume) (28) with immense internal surface area. The variety of Metal-ions ( $\text{Fe}^{2+}$ ,  $\text{Co}^{2+}$ ,  $\text{Ni}^{2+}$ ,  $\text{Cu}^{2+}$ ,  $\text{Zn}^{2+}$ ,  $\text{Mg}^{2+}$ ,  $\text{Mn}^{2+}$ ,  $\text{Al}^{3+}$ , and  $\text{Fe}^{3+}$ ) merged with different linkers results in the formation of variety of MOFs which can be used for numerous applications. The structures of these linkers remain undamaged after incorporation. In the past decade almost 20,000 MOFs are synthesized and studied. Previously MOFs were formulated with single-metal-ion nodes. In the preparation of MOF, selection of solvent is considered on the basis of properties of desired MOF. Nowadays, solvents such as ethanol, water and ionic solutions are popular for green MOF synthesis to reduce the toxic solvents usage (27).

## 2.1 MOFs and their antibacterial behavior

MOFs are excellent antibacterial agents due to their properties of having metal ions, reactive oxygen species (ROS) and interrupting the bacterial cell membrane. MOFs have tunable structure by addition of different ligands and antibiotics in their porous and crystalline structure which makes them suitable for ocular therapy. Most common MOFs used in terms of eye treatments, such as, ZIFs (metal ion release makes it effective to apply in contact lens besides hydrogel to inhibit bacterial growth), Ag based MOFs (silver ions are well known antimicrobial agents which impedes the microbial DNA replication), MOFs loaded with drugs (MOFs such as MIL-100 was loaded with ciprofloxacin for controlled and effective drug release) and Cu-MOF (copper ions has specialty of inducing oxidative stress to kill bacteria(29)).

## 2.2 Manufacturing of MOF

In past ten years, there have been numerous procedures to formulate metal organic frameworks. Few of them are listed below including formal methods long with advance and easy schemes (fig.6).

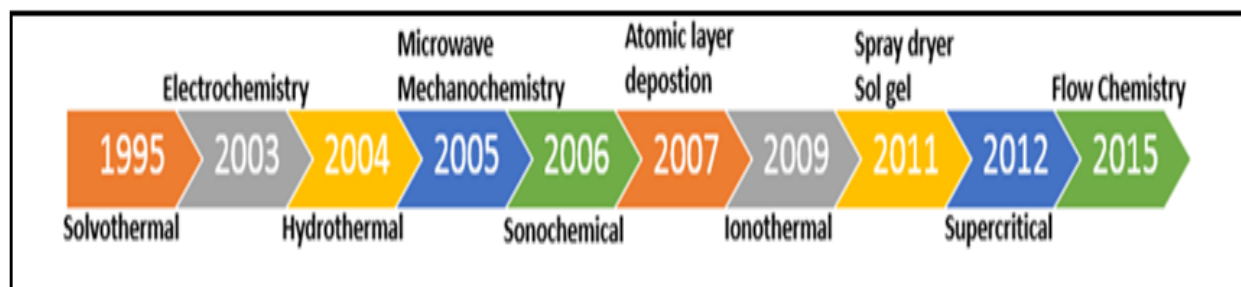


Figure 6- Overview of multiple MOF synthesis methods

### -Electrochemical synthesis

In 2005, company BASF holds the first patent to take advantage of synthesizing MOFs using electrochemistry. As in electrochemistry, electrical current has applied to examine the chemical changes. Researchers from this company formulated MOF with solution of 1,3,5-benzenetricarboxylic acid (BTC) as an organic linker having copper plates (for Cu ions source)

and electrolyte immersed in it. The octahedral crystals of MOF synthesized by this process was HKUST-1 having  $1820 \text{ m}^2\text{g}^{-1}$  surface area, higher than the surface area of HKUST-1 synthesized by solvothermal procedure. This synthesis took 150 minutes which got great attraction than conventional microwave or solvothermal process as it can take several hours or days to complete the procedure.

Electrochemical synthesis according to BASF patent consist of anodic dissolution. During anodic dissolution, metal ions released from electrode due to applied voltage. These metal ions then react with organic linker to form a MOF. Examples of MOFs synthesized by this process are Zn and Cu- carboxylates, Zn-imidazoles, HKUST-1, etc. (fig.7) (30) .

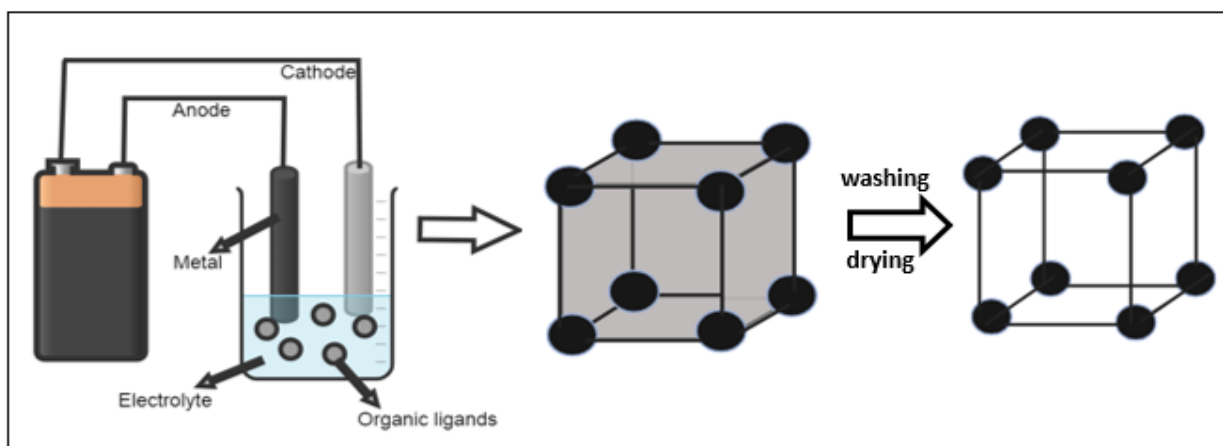


Figure 7- General scheme of electrochemical MOF synthesis.

### -Microwave synthesis

MOF can also be synthesized through microwave assisted method which utilizes electromagnetic waves and electric current (fig. 8). Polar molecules either in a solution or conducting ions in a solid, comes in direct contact with microwaves which makes this method more efficient in terms of heating. In solid heating is because of electric resistance and in solution, temperature increases due to the collision between polar molecules. MOFs synthesized using this method are Cr-MIL-100, Fe—MIL-100, Fe-MIL-101-NH<sub>2</sub>, MOF-177, Ni-glutarates, etc. (31).

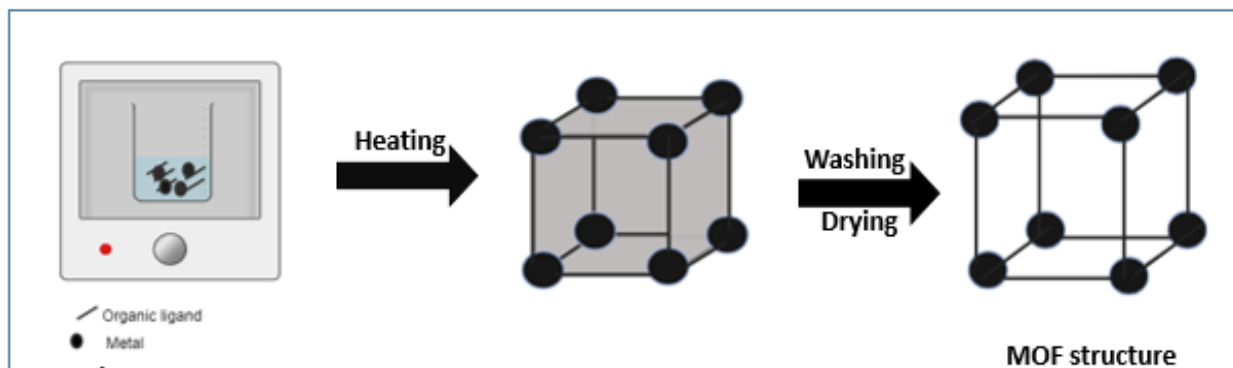


Figure 8- General illustration of microwave based MOF synthesis

## -Mechanochemical Synthesis

This process uses mechanophysics phenomena (such as milling or grinding) (fig. 9) to promote chemical reactions at room temperature. There are three ways of using this process to produce MOF; SFG- Solvent-Free Grinding (no solvent is used), LAG- Liquid Assisted Grinding (uses liquid to promote reagents mobility) and IAG- Ion and Liquid Assisted Grinding (liquid along with traces of salt). When hydroxides or oxides are used as a metal ion source in combination with organic ligand lead to form water as a byproduct is the main advantage of using this method. Examples of MOF prepared by this method are MOF-14,  $[\text{Zn}(\text{Elm})_2]$ ,  $[\text{Cu}(\text{INA})_2]$ , HKUST-1,  $[\text{Co}_3\text{C}_{16}(\text{L}')_2]$ , etc. (32).

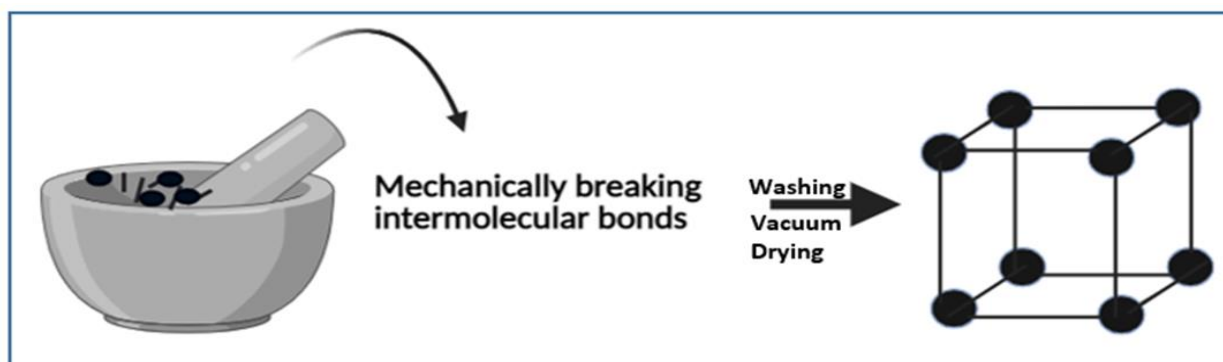


Figure 9- Mechanism for Mechanochemical synthesis of MOF

## -Solvothermal synthesis

This method utilizes protic (such as methanol, ethanol, etc.) or aprotic (such as DEF, DMF, DMSO, toluene etc.) organic solvents containing metal salts and organic linkers. In order to melt salt, this solution is heated at elevated temperature higher than the boiling point of protic or aprotic solvent. The conditions of high temperatures and autogenous pressure, yields large crystals with increased internal surface area (fig. 10).

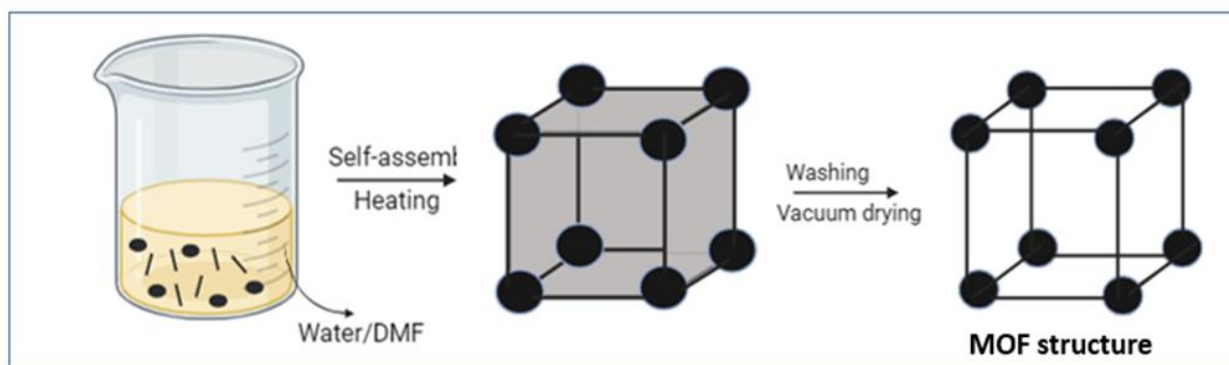


Figure 10- Mechanism for solvothermal synthesis of metal organic frameworks.

## 2.3 Examples of MOFs and applications

Table-1

Application	MOF	Metal	Ligand	Year
Drug delivery	MIL-101 [Cr <sub>3</sub> O(OH,F,H <sub>2</sub> O) <sub>3</sub> (1,4-bdc) <sub>3</sub> and MIL-100	Cr	1,4 bdc moieties or H <sub>3</sub> btc	2006 (33)
Antibacterial	Cu-BTC (MOF-199)	Cu	H <sub>3</sub> btc	2009 (34)
Highly potent bactericidal activity	Co-TDM	Co	H <sub>8</sub> tdm: tetrakis [(3,5-dicarboxyphenyl)-oxamethyl]methane	1989, (Terry Gullion, 1989)
CO <sub>2</sub> sorption	[Ni <sub>2</sub> (L-Asp) <sub>2</sub> (4,4'-bipy)].2H <sub>2</sub> O	Ni	L-Asp and 4,4'-bipy : 1,2-bis(4-pyridyl)ethane	2013 (35)
H <sub>2</sub> storage	MOF-177	Zn	4,4',4''-benzene-1,3,5-triyltribenzoate (BTB)	
Light-Emitting Diodes (LEDs)	Ln-MOF phosphors	Tb, Eu	BTC	2022, (36)
Nanomomedical applications	NO@HKUST-1@GO (NHGs)	NO	BTC	2021, (37)
Antibacterial	Ag <sub>2</sub> (O-IPA)(H <sub>2</sub> O).(H <sub>3</sub> O) and Ag <sub>5</sub> (PYDC) <sub>2</sub> (OH)	Ag	HO-H <sub>2</sub> ipa =5-hydroxyisophthalic acid and H <sub>2</sub> pydc= pyridine - 3,5-dicarboxylic acid	2014 (38)
Self-powered sensors	ZIF-7 TENG	Zn	Benzimidazole (BIM)	2020, (39)
Benzene detection sensor	MOF-14	Cu	1,3,5-tris(4-carboxyphenyl)benzene H3BTB	2020, (40)
Electrochemical enzyme-free sensor for H <sub>2</sub> O <sub>2</sub>	AuNPs-NH <sub>2</sub> /Cu-MOF	Cu	benzene-1,4-dicarboxylate (BDC)	2020, (40)

## 2.4 Classification of MOFs

Depending on the specific organic linker groups connected together to form MOF, classified in different categories having functional diversity. Octahedral MOFs formed by using [Zn<sub>4</sub>O]<sup>6+</sup> as sub-building units with aromatic carboxylates are termed as Isorecticular MOFs. Lately, nanosheets of IRMOF-3 has been used as a sensor in wastewater treatment for detection of 2, 4, 6-trinitrophenol (41). MOF consisting of Zeolite imidazole are categorized as ZIFs (Zeolitic Imidazolate Frameworks). These type of MOFs comprises of high porosity and stability. Some common ZIF includes ZIF-8, ZIF- 90, ZIF-7, etc. (42) .

Porous coordination networks (PCNs) are another class of octahedron MOFs employ in sensors owing to their hole-cage-hole geometry. Recurrent PCN MOF is PCN-222 MOF (42).

Materials Institute Lavoisier MOFs are utilized as a chemical sensors and synthesized with elements possess valence electrons combined with other compounds having carboxylic functional groups (43).

The MOFs having primary building unit of pyridine, carboxylic acid and their derivative and secondary building unit of transition metal, are termed as Porous Coordination Polymers (PCPs). These MOFs have properties which can be utilize in bio macromolecule separation and heterogeneous catalysis (44).

### **3. Introduction to Contact Lenses and Contact Lens Complications (CLC)**

Contact lenses (CL) were introduced in 19<sup>th</sup> Century, from then until now, is a prominent approach in thereabouts 41 million people worldwide (45) because of low cost, easy to handle and aesthetic purposes. In the past decade, 97% people wear contact lenses as specs substitute and not of medicinal or healing purposes (46). There are number of medicinal reasons also for wearing contact lenses, besides aesthetic purposes, for instance the correction of refractive issues, glaucoma, dry eye and eyesight improvement.

The benefits and convenience of contact lenses are accompanied by few complications. Impediments to the eyes due to contact lenses are termed as Contact Lens Complication (CLC) (47). CLC includes microbial keratitis, blepharitis, fungal infections, acanthamoeba keratitis, herpes simplex keratitis, herpes zoster keratitis and marginal keratitis (6).

Wearing contact lenses for the extended duration without taking proper cleaning measures, elevate the possibility of bacterial growth on it (48). Microorganisms cohere on the surface of CL and pass on to the outer surface or epithelial layer of eye resulting in Microbial Keratitis (MK). MK is specified for deforming the corneal epithelial layer in eye, which causes inflammation and severe pain. MK scarcely happens to healthy eyes (46).

Recurrent reasons of these diseases other than virulence of bacteria are usually the quality of life, resistance or immunity of the body, nutritional level, age group and physique (Joanna M. Willey, 2008).

This research majorly focused on Staphylococcus aureus (S. aureus) and Escherichia coli (E.coli), which are the significant bacteria in originating the eye infection. E.coli categorize as Gram-negative bacillus which exist as resident flora in human gut but pathogenic strains of E.coli can be found in human eye (49).

In 1885, Theodor Escherich described the gram negative anaerobic bacteria as E.coli. This bacteria are in common flora of gastrointestinal tract of both humans and animals. Despite that, these bacteria can be found in pathogenic strains which are competent to cause number of diseases in healthy person (50). Disease caused by pathogenic strains of E.coli includes ocular infection, corneal ulcer and endophthalmitis, hemolytic, pulmonary infections and Uremic syndrome. Eye related diseases includes conjunctivitis, keratitis, and dacryocystitis (51). Other than these antibiotics and traditional ophthalmic drugs, nowadays, contact lenses loaded with ophthalmic

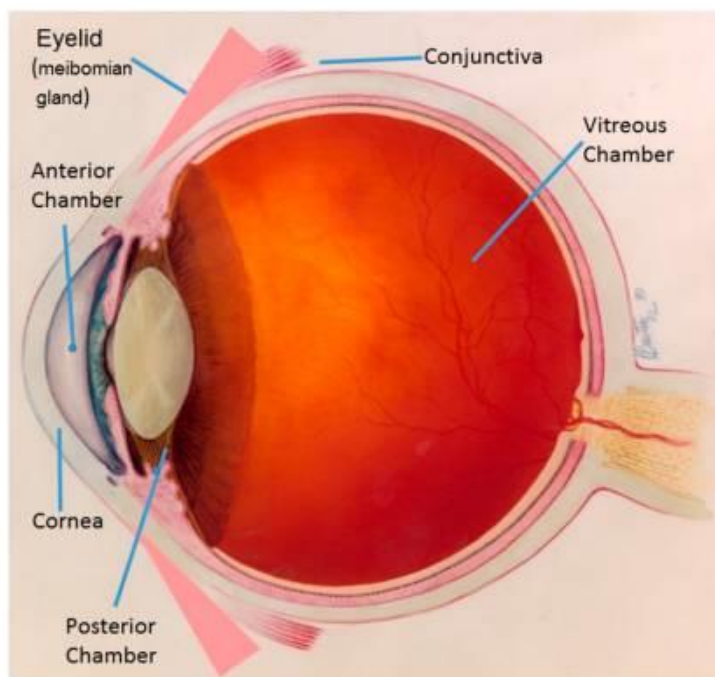


**Figure 11- Schematic representation of a human eye.**  
(O'Callaghan, 2018)

drugs are the best possible medical treatment devices. In 2013, scientists proved the effective coated CL with ciprofloxacin and dexamethasone by soaking it in acetate buffer and cyclodextrins (52). Another group of researchers in 2016, worked on the regular silicon contact lens by immersing in the moxifloxacin solution to observe the successful drug released (53). These soaking methods showed good drug release for initial few minutes but are not effective for long term treatment purposes.

### **3.1 Properties and Manufacturing of Contact lenses**

Typically, polymeric materials are used in contact lenses following different polymerization mechanisms (for e.g. radical vs catalytic polymerization) and conditions (such as temperature, initiator type, vessel used, etc.). There are broad range of contact lenses by varying the

manufacturing procedure but considering the factors with respect to materials science as mentioned in figure 12.

Considering the type of polymer, contact lens must have certain chemical properties such as wettability, oxygen absorption and water content. Wettability maintains a tear film to protect from dryness of contact lens. Another property of material of contact lens that it should pass oxygen through it. Water content in the lens keeps the CL hydrated (54).

These properties comprehends the comfort, eye response to the CL, friction between eyelid and CL and durability. These properties can be observed by strain generated due to implementation of stress on it (55).

The transparency and refractive index of polymer are the mandatory feature of polymer using for fabricating CL. The polymer should have refractive index of 1.37, same as of the cornea (55).

These type of contact lenses having pHEMA (poly 2-hydroxyethyl methacrylate) as a polymer, was the first soft CL. These contact lenses have network of cross linked hydrophilic polymers that allows the oxygen permeability (56). Silicone based contact lenses with hydrogels, are the fusion of hydrophobic and hydrophilic properties fused, and are also prevalent due to the comfort of hydrogel and high oxygen permeability of silicone (57).

CL with bactericidal lamination for instance silver nanoparticles, to lower the microbial keratitis percentage. Now a days smart contact lenses are also popular because of the integration of microelectronics and sensors for drug deliver and ocular treatment purposes (58). Regarding innovative materials, UV-blocking and Photochromic contact lenses are the examples. They are

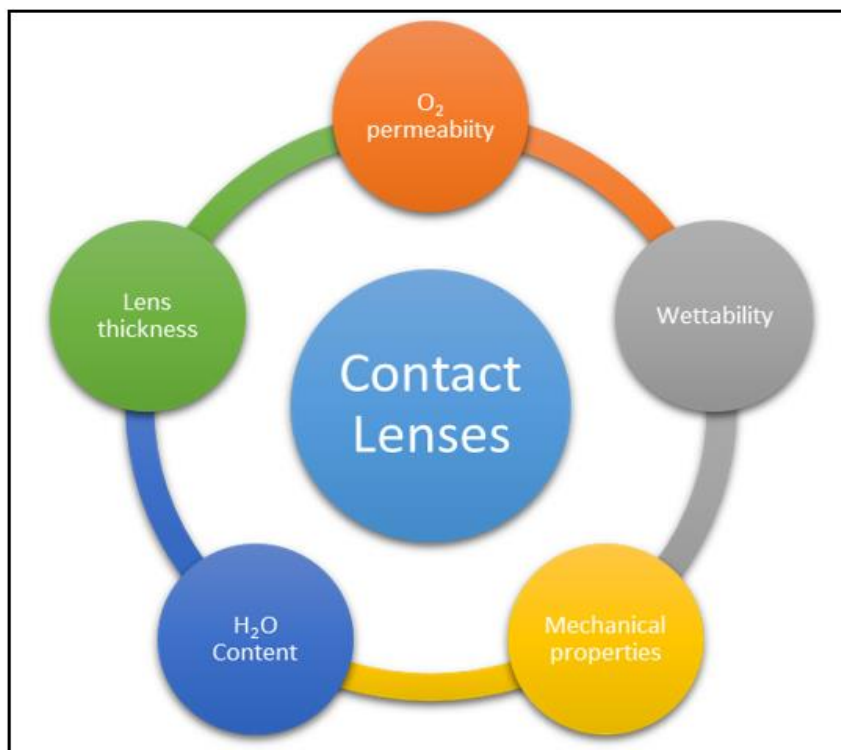


Figure 12- Conventional Properties of contact lenses

used for treatment and reducing the cataracts problem and additional UV related eye conditions (59).

#### 4. Drug loading technique on contact lens

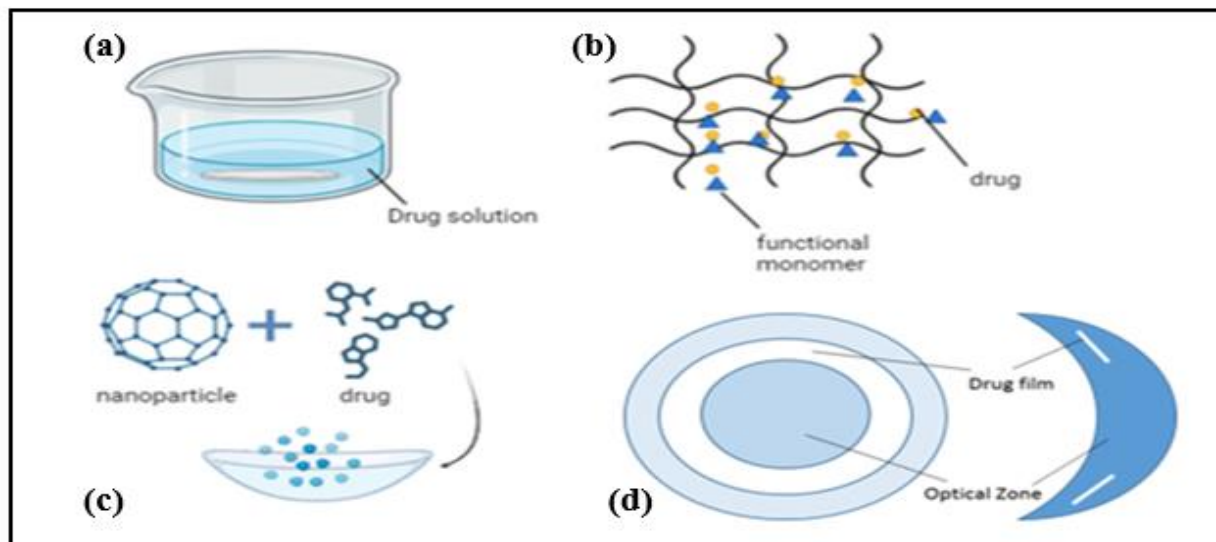


Figure 13- Techniques to load drugs on CL.

The drug delivery system is challenging because of the blood-eye barrier, preventing drug to absorb in the blood. This barrier is important in protecting the eyes, comprise of blood-water and blood-retinal barriers.

There are numerous ways to load antibacterial materials on CL which can target specific ocular tissues; molecular imprinting (MI) (60), soaking, composition alterations in lens and nanocarriers (Guzman-Aranguez, et al., 2016). For MI treatment, the drug is incorporated in the CL through etching of nanocavities which enhances the drug absorption. Drug can also absorb through soaking of CL in the drug solution which confines the medicine in the matrix of the CL (fig.13 (a)) The another way of drug delivery could be achieved by reforming the structure by adding binding sites on CL, such as methyl methacrylate was introduced to pHEMA lens to extend drug release period (fig.13(b)) (61). With the help of polymerization reaction functionalized nanoparticles are incorporated to enhance the time period of drug release, it is more feasible as compared to the soaking in nanoparticle solution(fig.13(c)) (62). Two matrixes are made inside the CL to incorporate polymer along with the layer of drug film for the purpose of better drug retention time (fig.13(d)) (63).

## 5. Antimicrobial resistance (AMR)

In 2019, there are around 4.95 million bacterial infections occurred worldwide which were drug resistant leading to 1.27million deaths, as reported in Global Research on Antimicrobial

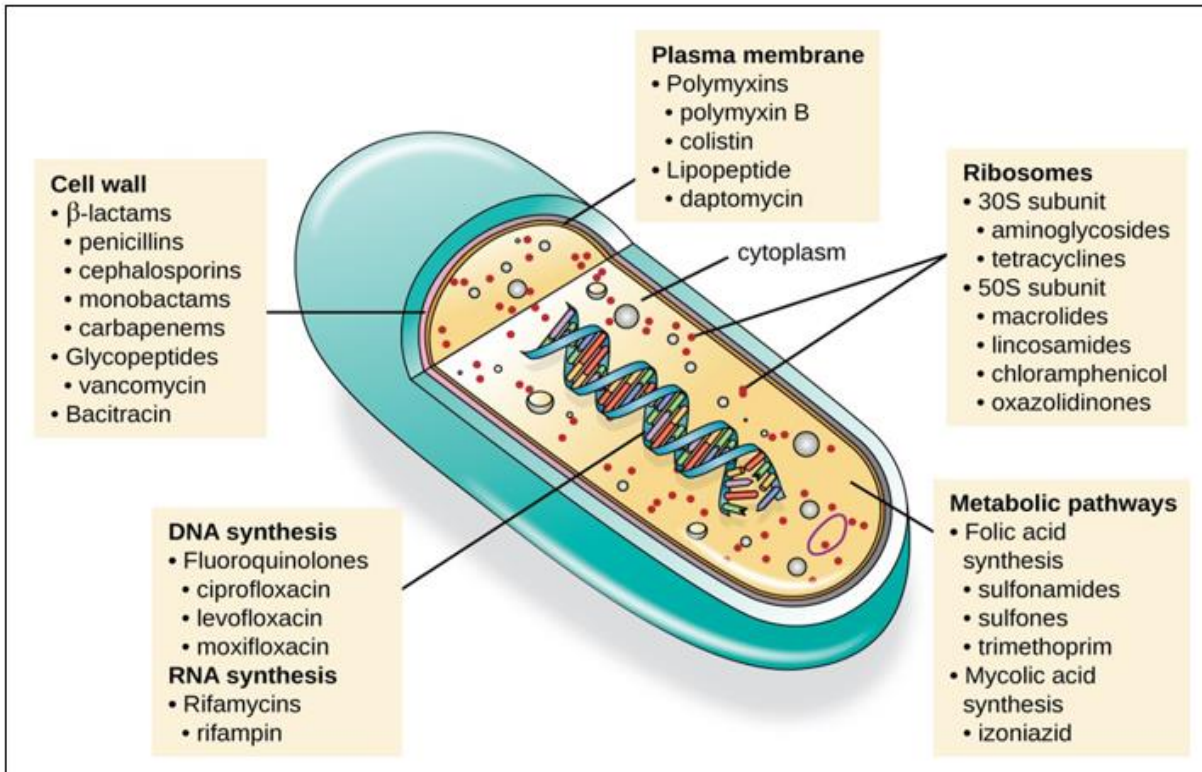


Figure 15- Target based classification of drugs. (Oregon State University, n.d.).

Resistance. This report also highlights that the Asian continent is majorly affected by the AMR (64). Antimicrobial resistance suggests that when bacteria fungi parasites don't retort to antimicrobial drugs, leaving the medicine ineffective which leads to difficulty in treating the disease. AMR effects not only health systems but also have ramifications on the country's economy.

The popular member of Gram positive and Gram negative bacteria are *Escherichia coli* (*E. coli*) and *Staphylococcus aureus* (*S. aureus*) respectively. *E.coli* can be found in normal human gut flora but is capable to cause grievous infections. There are various pathways through which these bacteria can attack on the human heath which includes contaminated water and food supply and direct contact with the carrier. According to research by group of scientists, *E.coli* is capable of over 50% resistance towards drugs such as penicillin, cepheims and teteracyclines. However, *S. aureus* bacteria can resist to 40% of penicillin's, lincosamides and macrolides medicines (Yan Guo, 2023). Other than *E.coli* and *S.aureus*, *Klebsiella pneumoniae*, also appeared to be resistant towards antibiotics, as Global Antimicrobial Resistance and Use Surveillance System (GLASS) report published in 2022 (65).

It is considered to be a natural or acquired phenomenon of bacteria to resist antibiotic. There can be couple of genetic mechanisms, including existing gene mutation and mutation in the individual

organism which help bacteria to resist from drug. This resistance formed in bacteria occurred from antibiotic itself. The excessive dosage or prolonged treatment with antiseptics or antibiotics makes the bacteria to combat against it after some period of time (66). Polymyxins can also attack on the bacterial membrane structure resulting in expanding the permeability of the membrane which in turn loses the bacterial content and eventually the death of bacterium. As each drug affects/target specific part of cell, table-2 summarizes the drugs and their mode of action. Fig.15 describes the outline of the various drugs and its targets.

**Table 2** (NEU, 1992).

<b>Mode of Action</b>	<b>Antimicrobial agents</b>
Interference with cell wall synthesis	$\beta$ -Lactams: penicillins, cephalosporins, carbapenems, monobactams —Glycopeptides: vancomycin, teicoplanin
Protein synthesis inhibition	Bind to 50S ribosomal subunit: macrolides, chloramphenicol, clindamycin, dalbavancin, linezolid Bind to 30S ribosomal subunit: aminoglycosides, tetracyclines Bind to bacterial isoleucyl-tRNA synthetase: mupirocin
Interference with nucleic acid synthesis	inhibit DNA synthesis: fluoroquinolones Inhibit RNA synthesis: rifampin
Inhibition of metabolic pathway	sulfonamides, folic acid analogues
Disruption of bacterial membrane structure	polymyxins, daptomycin

### 5.1 Gram-positive and Gram-negative bacteria

There are two broad classes of bacteria, categorized on the basis of cell wall structure. To determine the specific class of bacteria, staining method has been introduced by bacteriologist Hans Christian Gram in 1884. These staining procedures not only differentiate between bacteria but also deduce the structure and cell wall composition.

The gram positive bacteria is surrounded by single cytoplasmic membrane (monoderms, contains lipoteichoic acids) covered by peptidoglycan layer (20-8-nm, contains teichoic acid). On contrary, gram negative bacteria have intricate cell wall structure (diderms- inner and outer membranes) (fig.16). It consist of cytoplasmic membrane, peptidoglycan layer (2-7nm) and outer membrane containing lipopolysaccharides.

In order to detect the speciality of bacteria, gram staining test has been done by using specific dyes. Crystal violet dye is used for staining purposes. Gram positive bacteria keep the violet color by forming dye and iodine complex structure which is not easy to breakable during alcohol washing.

However the gram negative bacteria, having thin peptidoglycan layer structure, cannot hold violet color from dye and dye easily washed away from alcohol. Therefore, it appears pink as a result of gram staining (67).

**Table 3-** List of gram positive and gram negative bacteria

Gram positive bacteria	Gram negative bacteria
<i>Staphylococcus aureus</i>	<i>Salmonella typhi</i>
<i>Staphylococcus epidermidis</i>	<i>Salmonella typhimurum</i>
<i>Staphylococcus saprophyticus</i>	<i>Pseudomonas aeruginosa</i>
<i>Aspergillus niger</i>	<i>Chromobacterium violaceum</i>
<i>Enterococcus durans</i>	<i>Proteus mirabilis</i>
<i>Listeria monocytogenes</i>	<i>Shigella flexneri</i>
<i>Micrococcus luteus</i>	<i>Salmonella infantis</i>
<i>Bacillus subtilis</i>	<i>Proteus vulgaris</i>
<i>Enterococcus faecalis</i>	<i>Pseudomonas fluorescens</i>
<i>Methicillin Resistant Staphylococcus aureus</i>	<i>Salmonella enteritidis</i>
<i>Bacillus cereus</i>	<i>Klebsiella pneumonia</i>

(68), (69)

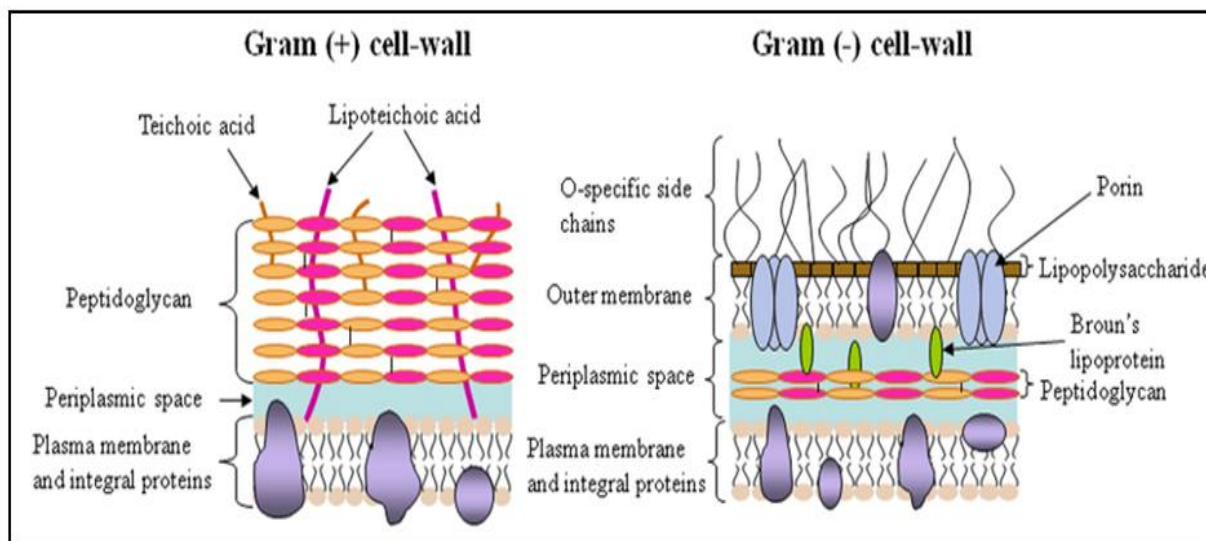


**Figure 16-** Gram positive and negative cell wall structure (Atanasova, 2010)

## 6. Composites used for antimicrobial purposes

There are considerable methods and materials developed to overcome the problem of bacterial infections and diseases. Starting from nature based agents, metals (Ag, Cu, Ti), Hydroxyapatite, Ag-phosphate, AgNPs, metal oxides, Chitosans, polymers, carbon based nanomaterials ceramic materials etc.

**Table 4- List of Nature based Antimicrobial agents**

	<b>Major component</b>	<b>Target bacteria</b>	<b>References</b>
<b>Plant Based</b>	Phenolics and flavonoids	S.aureus, E.coli, Yersinia	2014, (70)
	Tannins	MRSA ATCC 43300 and E.coli ATCC 35218	2007, (71)
	Polyphenolic compounds	S.aureus, P.fluorescens	2014, (70)
	Polyphenols	S.aureus, L.monocytogenes	2010, (72)
	Phytochemicals	E.coli O157:H7, Shigella sonnei	2003, (73)
	Betacyanins, betaxanthins	B.cereus, P.aeruginosa	(Antioxidant and antimicrobial activities of beet root pomace extracts, 2011)
<b>Animal based</b>	Glycoprotein	<i>L. monocytogenes, Salmonella</i>	2024, (74)
	Eicosapentaenoic acid (EPA) and Docosaheptaenoic acid (DHA)	<i>E. coli, B. subtilis, Pseudomonas aeruginosa, S. Enteritidis, S. Typhimurium</i>	2007, (75)
	cationic peptides	Gram-ve and +ve bacteria	2009, (76)
	Glutamic acid, aspartic acid	<i>Micrococcus, L. monocytogenes</i>	2024, (77)
	Bioactive peptides	<i>Enterobacter sakazakii</i> ATCC 12868	2020, (78)
<b>Bacterial origin</b>	Nisin	<i>Clostridium</i> spp., <i>L. monocytogenes</i>	2012, (79)
	Lactocin	<i>E. coli</i> strains	2007, (80)
	Acidophilin	<i>Listeria ivanovii, B. cereus</i>	2013, (81)
	Plantaricin	<i>L. monocytogenes, S. aureus, S. Typhimurium, E. coli</i>	2010, (54)
	Helveticin	<i>Clostridium botulinum</i>	2002, (82)

### **Antimicrobial materials**

The most common agent used in CL is polyquaternium-1(PQ-1) which works by combining with negatively charged bacterial cell wall due to electrostatic interaction leading to cell death. This is effective against wide range of bacteria including Staphylococcus aureus and Escherichia coli. The

prolong usage of this drug creates resistance in the bacteria by reducing the reactivity towards PQ-1.

Another antibacterial drug, chlorhexidine, has been used in the manufacturing of contact lens along with hydrogel. The chlorhexidine attacks on the bacterial membranes and cause leakage in cytoplasm. However, this drug has significant limitations such as higher concentration damages the epithelial cells of eye and low solubility in hydrogel restricts its use in CL.

Fluoroquinolones are able to utilize in CL to treat eye infections by attacking on DNA which in turns inhibit replication. The CL loaded with fluoroquinolones face challenge of rapid drug release and bacterial resistance also increased by overdosing.

**Ceramics** - Ceramics can be operated as microbicidal agents due to the properties of biocompatibility and thermal stability. When metal ions, such as silver ions, are merged in ceramics matrix facilitates the ROS (Reactive Oxygen Species) generation and cell wall disruption. Silver based ceramics are demanding antibacterial agent, implied as a coating on CL to minimize the bacterial growth. Moreover, silicon nitride and zirconia also show high antibacterial activity and widely used as coatings (83).



Figure 17- Drug discoveries over the years.

**Carbon based Nano materials as antimicrobial agent** - These materials have specialty of high surface area, tunable surface which makes them highly suitable for antibacterial activity. Carbon based nanomaterials include graphene, fullerene, carbon quantum dots, graphene oxide and carbon nanotubes (fig. 20). The mechanism of these agents to kill bacteria, primarily consist of ROS generation. The physicochemical property of graphene, having sharp edges, also helped for the bactericidal activity proceeding to the disruption of cell membrane. These agents can produce ROS in the presence of light which holds the potential of DNA damage and its application in PDT (Photo Dynamic Therapy). Despite small size of carbon quantum dots, they have good control in penetrating and then interacting with microbial membrane and its components. The surfaces of these nanomaterials can be tuned with functional groups to enhance its properties (84).

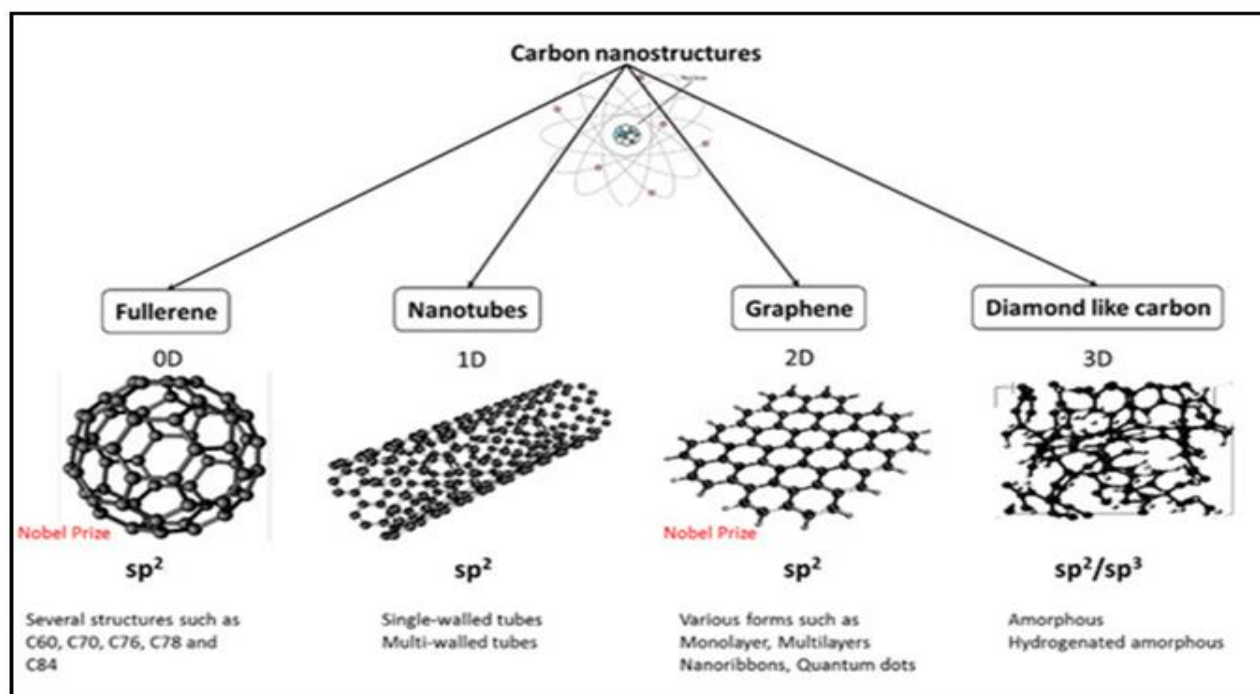


**Figure 20- Overview of carbon based bactericidal agents.** (Solmaz Maleki Dizaj 1, 2015)

**Metal ions as antimicrobial agents** - Metals such as silver, copper, zinc, gold, and iron manifests antimicrobial activity not only for bacteria but also for fungi and viruses. Other than Metal ions, they can be work in the form of oxides, salts and nanoparticles. The mechanism of their bactericidal behavior varies from metal nature. For instance, Silver ions along with functional group of proteins (thiol), suspend the metabolic activities and hinder the replication of DNA of bacteria (85). Copper and zinc ions follows the oxidative stress (producing hydroxyl radicals) rule to inhibit bacterial growth. Gold ions itself is less reactive but effective when coupled with other functional groups or agents (86). Gold nanoparticles can produce ROS on exposure to light to kill bacteria (87). Furthermore, titanium dioxide is also prominent candidate in the list of antimicrobial agents, inhibiting bacterial growth by ROS generation.

**Chitosan antimicrobial agents** - Chitosan are biopolymer, chitin derived polysaccharides. They are formulated by deacetylation of chitin. Chitosan possess excellent antibacterial effect by opposite charge interaction, means negatively charged chitosan combine with positively charged cell membranes which ultimately results in the decomposition of cell. Researchers reported that chitosan can behave as antibacterial agent for both positive and negative bacteria. It hinders the biofilm formation and also able to bind with metallic ions. CL are coated by layer of chitosan using dip-coating or layer-by-layer assembly. The challenges faced in the coating are friction, durability and transparency of this material (88).

**Synthetic Polymers as antibacterial agents** - Synthetic Polymers can served as bacteria killing agents because of its unique properties, for instance, having cationic charges to easily attract bacterial cell membrane. Quaternary ammonium compounds (QACs), polyhexammethylene, Antimicrobial peptides (AMPs) and N-halamines (89). These polymers denatures the microbial cell protein directing to the cell death. Other polymers including poly(2-(dimethylamino)ethyl methacrylate) (PDMAEMA) and polyethylenimine (PEI) also emerged having effective bactericidal properties (90).

## 7. Materials and Methods

### 7.1 Materials

MAX powder ( $Ti_3AlC_2$ ) was purchased from Aladdin Chemical Reagent Co., Ltd. (Shanghai, China). Hydrochloric acid, Lithium fluoride, Copper nitrate trihydrate, Zinc nitrate hexahydrate, methylimidazole, ethanol, Lithium phenyl 2,4,6 trimethyl benzoyl phosphate(LAP) and hyaluronic acid methacrylate (HAMA) was purchased from Chemical Reagent Co., Ltd. (Shanghai, China). Ultra-pure deionized water (DI) was used as a solvent. MXene was synthesized according to the procedure mentioned below.

### 7.2 Characterizations Studies

The morphology and atomic arrangements were measured using FEI Inspect F50 (USA) scanning electron microscopy (SEM). In this imaging, Secondary Electrons (SE) signals are obtained to observe the sample's surface morphology and texture at nanoscale. The lamellar distancing between layers and crystal structure was analyzed using X-ray diffraction (XRD) (Aeris PAN analyticals benchtop diffractometer). For XRD the sample was coated with copper (due to its negligible background noise) and analyzed in slow scan mode using  $Cu K\alpha$  source. The surface properties of MXene and composite were measured using TEM (JEM-2100F instrument (JEOL, Japan). The composition, surface groups, and intercalated species were analyzed by using FTIR spectroscopy (PerkinElmer Spectrum Two FT-IR Spectrometer) having range of  $8300 - 350\text{ cm}^{-1}$ . In this technique lithium tantalite NIR detector has been used.

### 7.3 Preparation of $Ti_3C_2T_x$ -MXene

A stock solution of 6M HCl (30 ml) was equally divided into two PTFE bottles. To each of these bottles, 750 mg of LiF was added and stirred in a pre-heated oil bath at  $45\text{ }^\circ\text{C}$ . Once all the LiF is

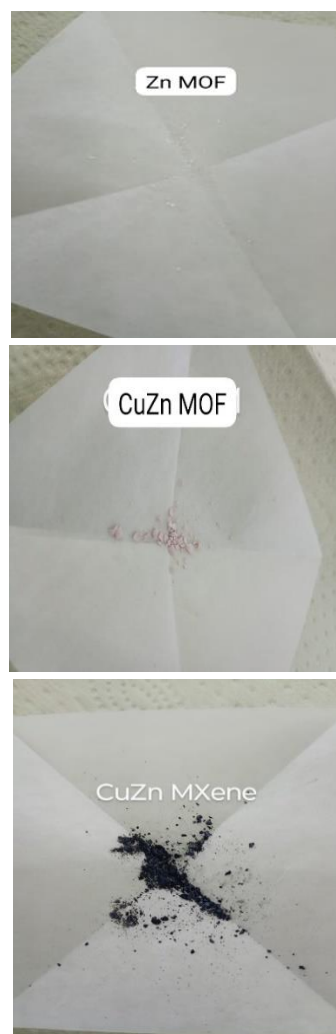
dissolved (~5 mins), 750 mg of  $Ti_3AlC_2$  was then slowly added to each bottle over a course of 5 min. After loosely capping, the mixture was stirred for 48 h at 45 °C. After completion of the reaction, the mixture was cooled to room temperature followed by multiple rounds of centrifugation with DI water until the pH of the supernatant becomes >6. The wet slurry was then dispersed in DI water and collected using vacuum-assisted filtering followed by drying at room temperature under vacuum in a desiccator for 24 h (fig.21).

#### 7.4 Preparation of CuZn MOF MXene composite

**Zn-MOF** – 53.56mg of  $Zn(II) (NO_3) \cdot 6H_2O$  was mixed with 5ml methanol in a vial (a). In separate vial (b), 65.68mg 2-methylimidazole was taken with 5ml methanol. Both solutions (a) and (b) were thoroughly mixed on a magnetic stirrer. Solution from vial (a) was added drop by drop into vial (b). The final solution was kept on stirrer for 12 hours. The precipitates formed in the solution were then centrifuged at 10,000 rpm and then dried in oven at 65 degrees to obtain Zn-MOF.

**CuZn-MOF** – In 5ml methanol solution, 39.65mg of  $Zn(II) (NO_3) \cdot 6H_2O$  and 16.10mg of  $Cu(II) (NO_3) \cdot 3H_2O$  were mixed (Solution a). 65.48mg methylimidazole solution was prepared in 5ml methanol (solution b). Both solutions (a) and (b) were combined and same steps were followed as mentioned in Zn-MOF preparation.

**CuZn MOF MXene** – Solution (a) was prepared containing 39.48mg  $Zn(II) (NO_3) \cdot 6H_2O$ , 16.73mg  $Cu(II) (NO_3) \cdot 3H_2O$  and 15 mg of MXene were mixed thoroughly on magnetic stirrer. For Solution (b), 65.23mg Methylimidazole was homogenized with 5ml methanol.



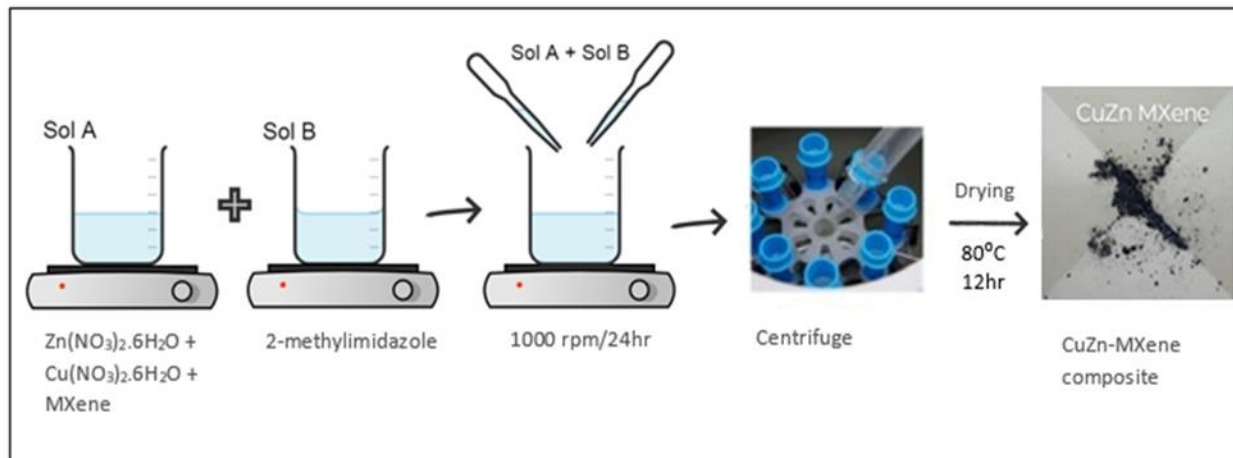


Figure 21- Illustration of synthesis of CuZn MOF MXene composite

**7.5 Preparation of bacterial Culture** - To revive bacteria, Luria-Bertani (LB) nutrient culture was prepared using 8g of LB with 400ml of distilled water in a glass bottle and was placed in autoclave for 2 hours at 121°C. Later, 10-15ml LB was taken in a sterile plastic tube. Small amount of bacteria was taken in the LB tube, using inoculation loop from already grown bacteria. The tube was placed on shaker for even distribution of bacteria. Afterward, the LB tube was placed for incubation at 35°C for 12 hours. The bacterial growth can be seen from the turbidity of the medium. The bacterial growth was confirmed on solid medium also using the same liquid bacterial media (fig.21). For antibacterial experiment, first bacterial colonies were grown in 96 well culture plates (fig.21 a) and incubated for 12 hours at 37°C. Thereafter, each concentration from well plate, was diluted four times using 900µl Phosphate Buffer Solution (PBS) and 5µl well plate media. Few drops (2-3 µl) of diluted bacterial culture was placed on nutrient agar plates.

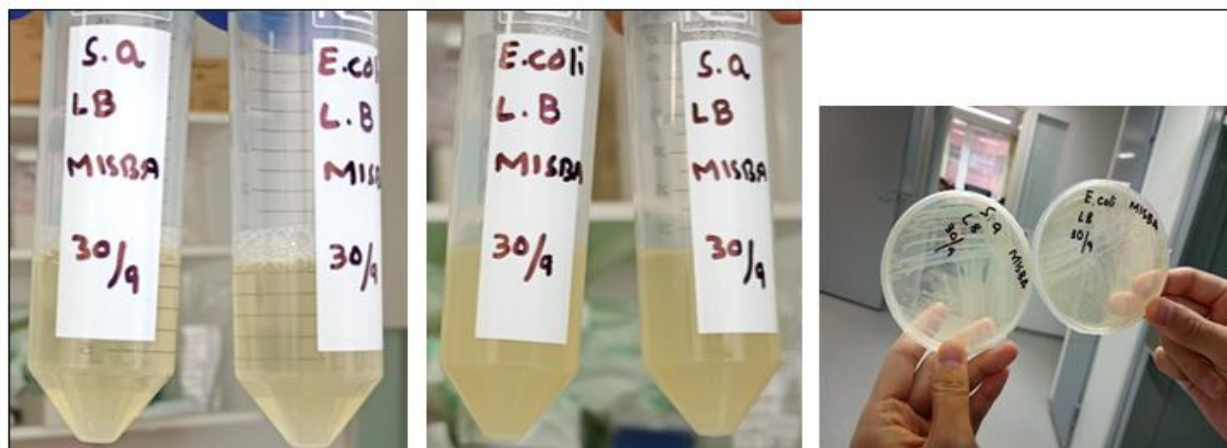


Figure 21- Preparation of LB culture before and after incubation, petri plates with E.coli and S.aureus bacteria.

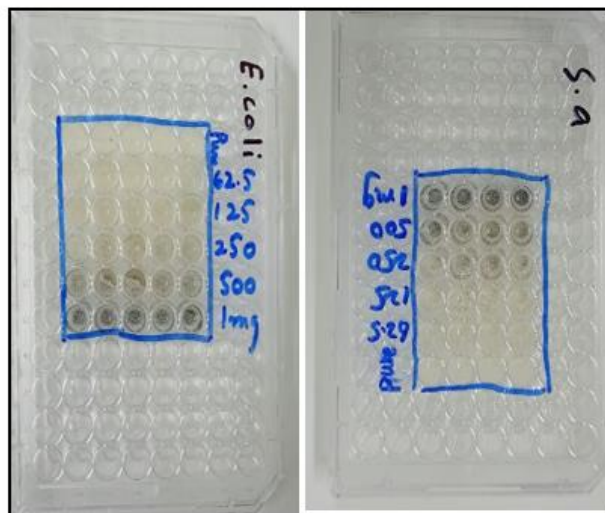


Figure 21(A) - 96 well culture plates

## 7.6 Negative results

Initially, 2mg/ml, 1 mg/ml, 500 $\mu$ g/ml, 250  $\mu$ g/ml, 125  $\mu$ g/ml and 62.5  $\mu$ g/ml concentrations of MXene and CuZn MOF were used to examine the antibacterial properties. After the treatment of bacteria with these concentrations, results were not as per literature. The 2mg, 1mg, 500, 125 and 62.5  $\mu$ g/ml concentrations did not worked well to inhibit bacterial growth (fig.21-b). The main reasons for the limited bactericidal activity of these concentrations could be the use of degraded/oxidized MXene and the low concentrations of MXene and high concentration of bacteria used initially in this research work. The oxidized MXene effect on the mutual behavior. Of CuZn MOF and MXene.

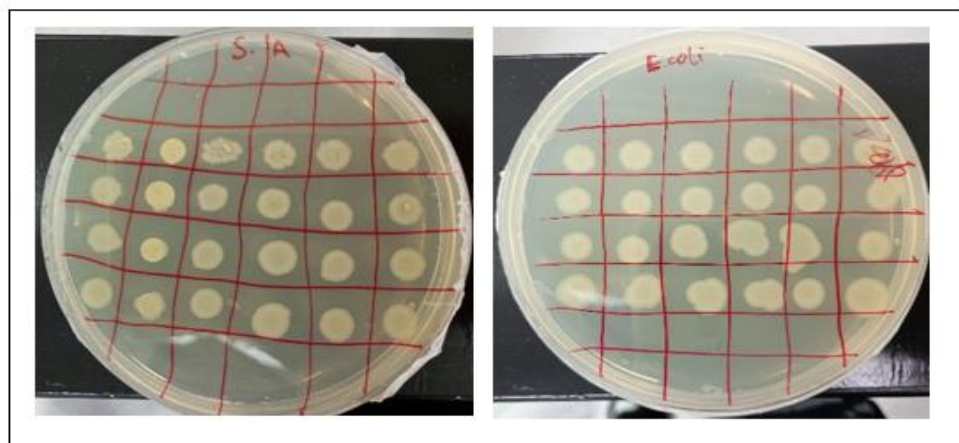
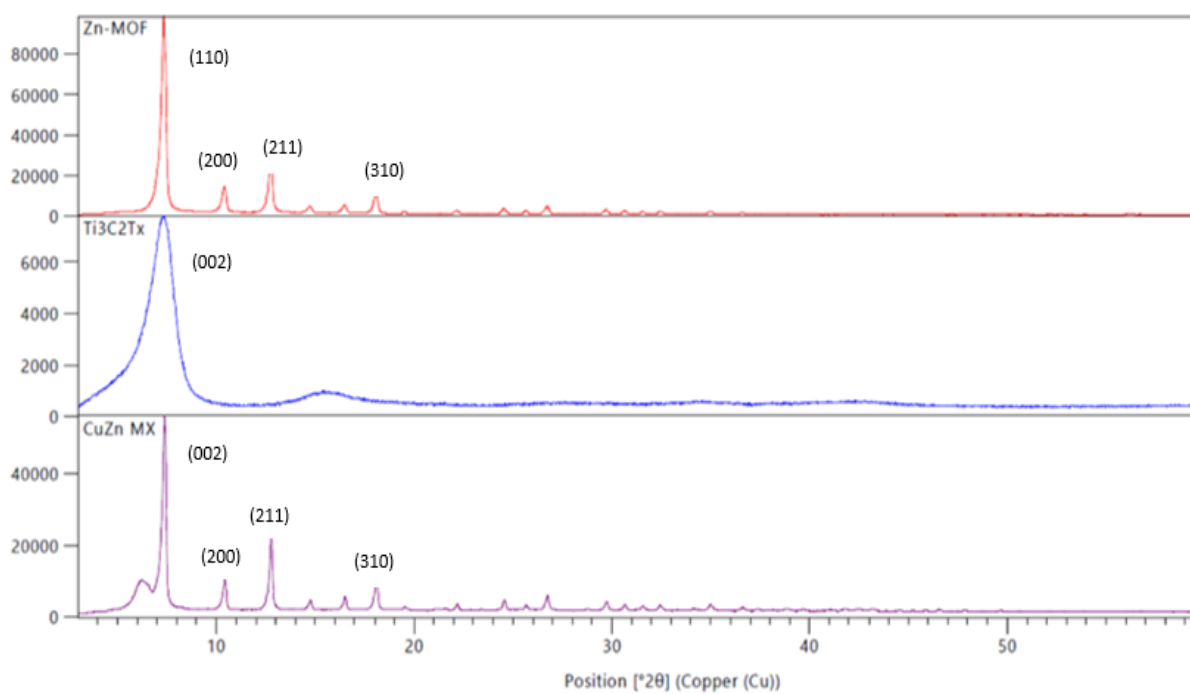


Figure 21(b) - Failed results of CuZn MOF MXene composite with *E.coli* and *S.aureus* bacteria.

## 8. Results

### 8.1 XRD analysis

This technique is done to determine the crystal lattice structure of a given sample. This is an x-ray diffraction method. When x-ray falls on parallel planes of sample they will reflect that light and perform constructive and destructive interference. The intensities and theta, due to interference, will define the structure of the sample. Shift in peaks shows homogeneous strain while broadness of peaks shows heterogeneous strain. In CuZn MOF MXene composite the characteristic peak of MXene at  $7.5^\circ$  on the 002 plane, corresponds to the interlayer spacing of 1.18nm in MXene and



**Figure 22- XRD analysis of Zn MOF, MXene and CuZn MOF MXene**

also visible in CuZn MXene composite. In ZIF-8, peaks at  $7.1^\circ$ ,  $10.2^\circ$ ,  $13.0^\circ$  and  $18.4^\circ$  corresponding to the (110), (200), (211) and (310) planes respectively (fig. 22) (91). These peaks exhibit good crystallinity of Zn-MOF and also matched with the literature (92). The sharp signals of Zn-MOF in the CuZn composite indicates the successful formation of multifaceted structure of this composite. The similarity in the peaks specify that the introduction of copper ions did not affect the crystal structure of ZIF-8 MOF (no changes can be due to similar ionic size of  $\text{Cu}^{+2}$  and  $\text{Zn}^{+2}$ ).

## 8.2 FTIR analysis

FTIR spectroscopy provides information about composition and structure of sample and the changes in chemical bonds by absorption of infrared light. This composite shows peak at  $494\text{cm}^{-1}$  indicating the presence of Cu-N bond of Cu-MOF in the composite (93). The stretching vibration band at  $420\text{cm}^{-1}$  shows the formation of Zn-N of imidazole of Zn-MOF. The Ti-C peak at  $594\text{cm}^{-1}$  from  $\text{Ti}_3\text{C}_2\text{T}_x$  MXene and -OH group presence can be seen from weak peaks ranging from  $3000\text{cm}^{-1}$  to  $3500\text{cm}^{-1}$ (fig. 23).

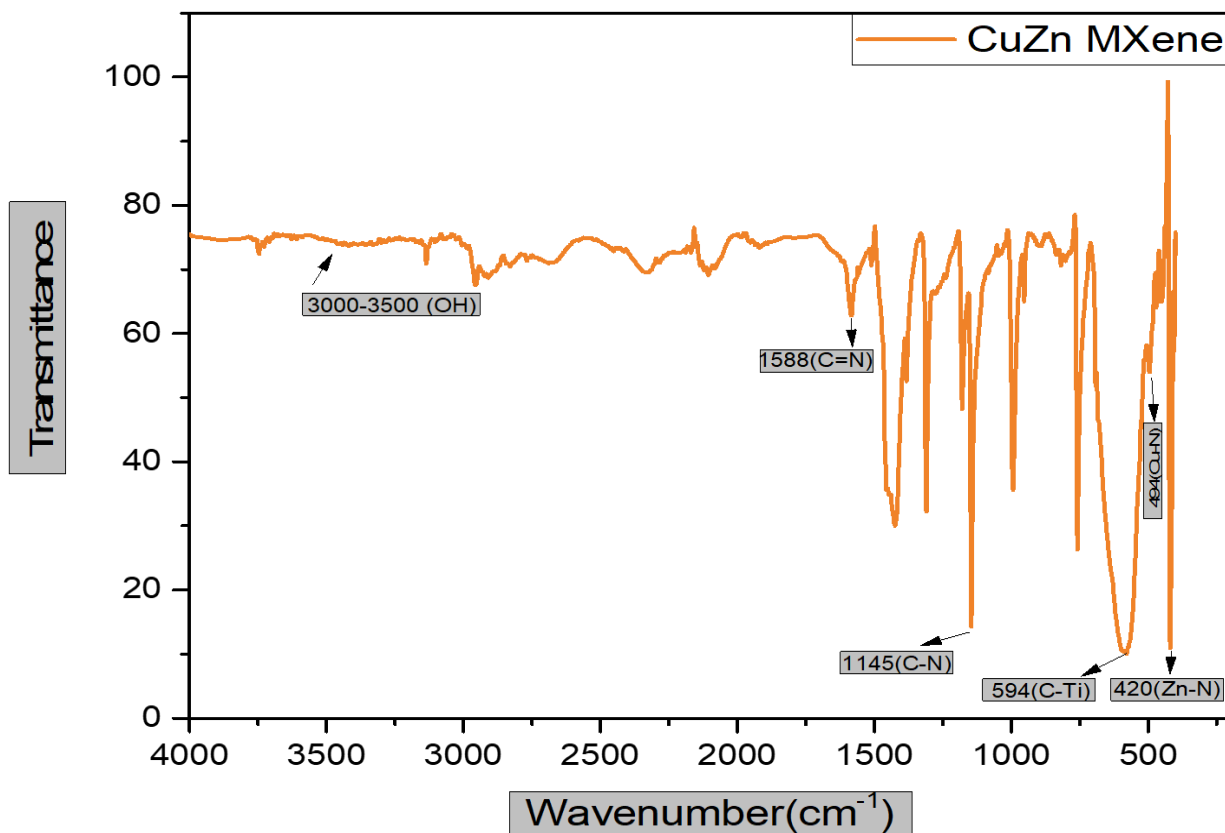
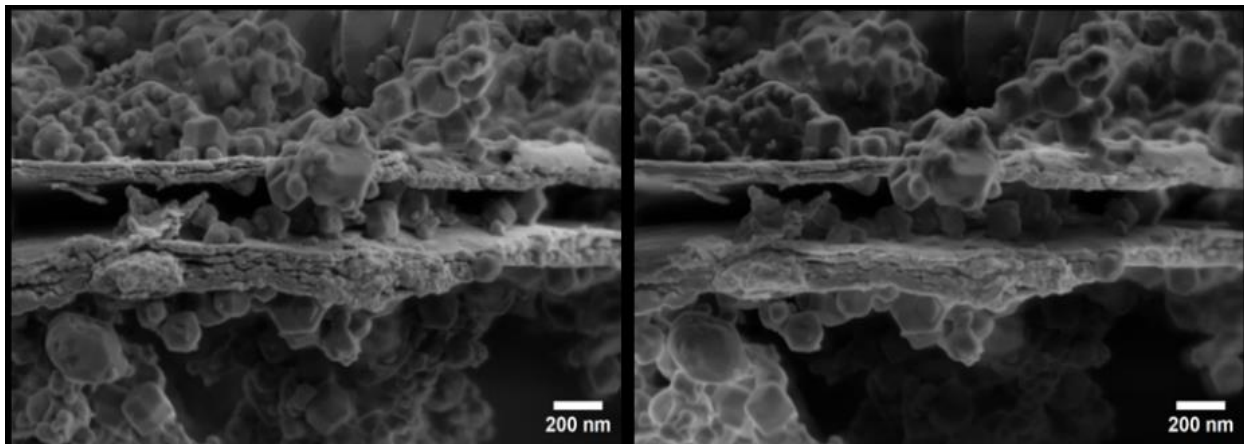


Figure 23- FTIR-ATR analysis of CuZn MOF MXene composite.

### 8.3 SEM Imaging

Scanning Electron Microscopy is the technique used for analyzing samples using electrons instead of light to form an image. It measures structural components and surface morphology. SEM analysis of this composite showed the clear lamellar structure of MXene loaded with CuZn MOF between and surrounding of the layers (fig. 24). The typical rhombic shape of Zn-MOF (ZIF- 8) is visible, along with clusters of Cu MOF, concluding the successful formation of CuZn MOF (fig. 25).



*Figure 24- SEM imaging of MXene layers decorated with CuZn MOF.*

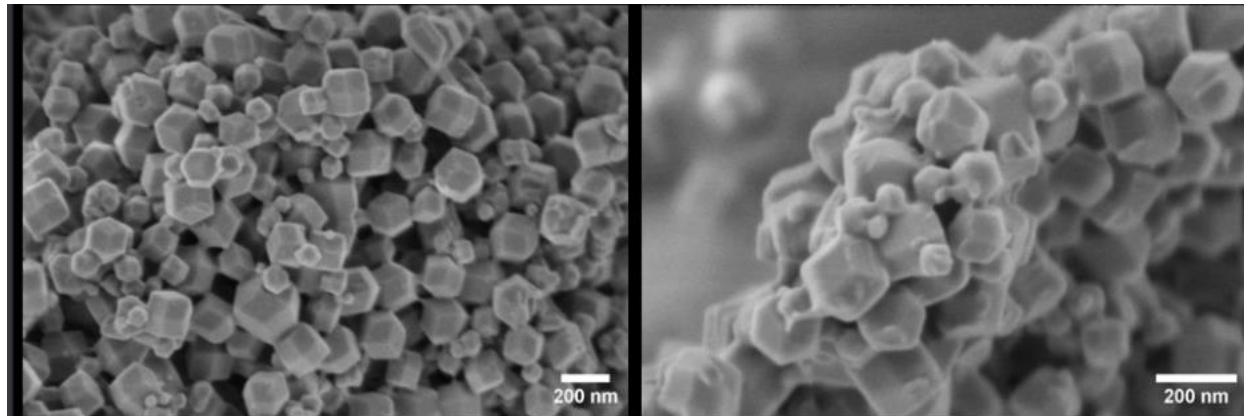


*Figure 25- SEM images of CuZn MOF.*

## 8.4 TEM imaging

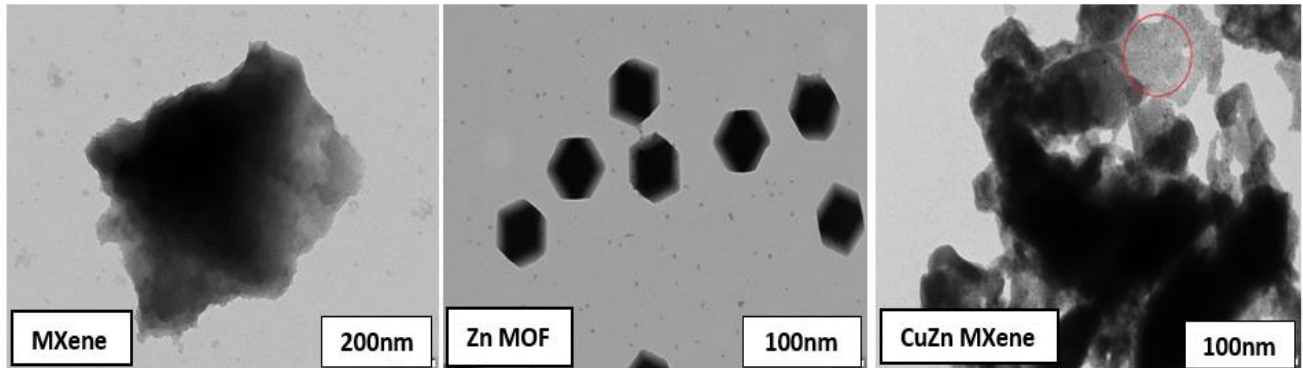


Figure 26- Analysis of CuZn MOF MXene composite under transmission electron microscopy.

This technique shows the crystal structure, morphology, chemical composition and defects of the composite by using electron beams which passes through the sample and forms an image on the computer. For this composite, Zn MOF has similar hexagonal structure with smooth borders at 100nm as mentioned in the literature (94). The MXene TEM analysis shows good thickness of approximately 1-2 nm and stacked layers at 200nm (fig. 26). To conclude, the CuZn MOF MXene shows porous morphology and proper addition of MOF with MXene.

## 8.5 Antibacterial analysis

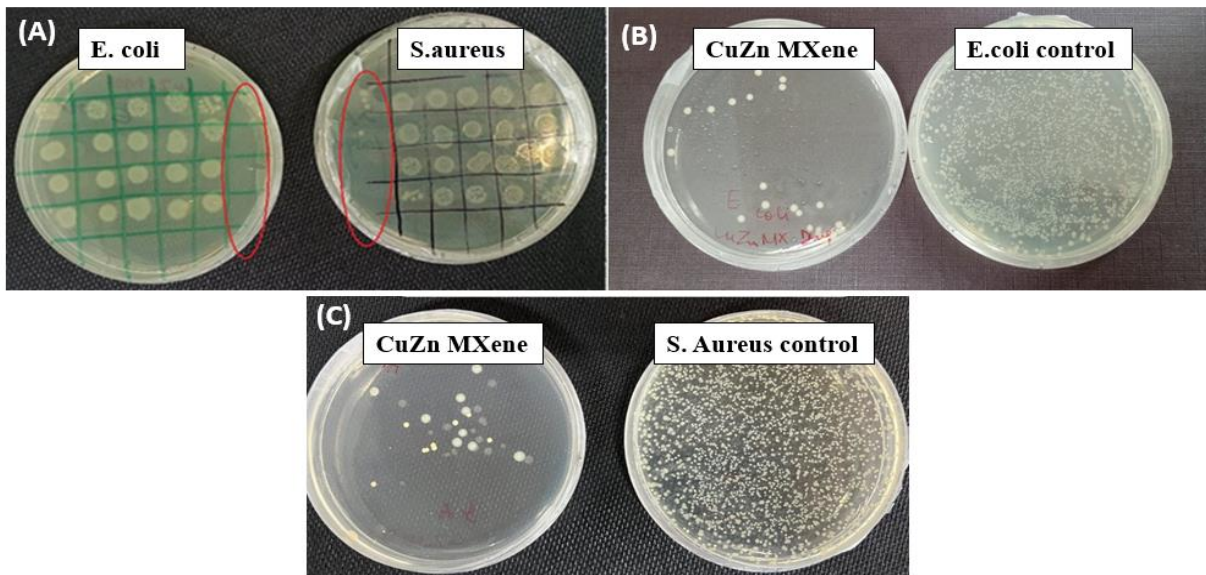


Figure 27- Antibacterial experiments with CuZn MOF on E.coli and S. aureus (A), CuZn MXene was introduced with both bacteria and their control (B and C).

Bactericidal test was done by growing microbial colonies of E.coli and S. aureus on agar plates after 12 hours of inhibition at 37°C. The figures 27(A-C) shows antibacterial effect of this composite. In fig. 29(A) the CuZn MOF was treated with both bacteria and the inhibition of bacterial colony is highlighted. In fig. 29(B-C) the agar plates marked control are full of bacterial

colonies as compared to the other plate having the composite showing 98% bacterial growth inhibition.

## 9. Contact lens formation

CL can be prepared by using Polymethyl methacrylate (PMMA) and Rigid Gas Permeable lenses (RGP) uses fluorosilicone acrylate for the formation of typical hard CL. Hydrogel based lenses are synthesized from Polyhydroxymethyl methacrylate (pHEMA), Silicone hydrogel based lenses (hydrogel polymer such as senofilcon A) and hybrid lenses (hard center and soft outer ring) fall in the category of soft CL.

Contact lens were made during this research using cross linker polymer 8mg, Lithium phenyl 2,4,6 trimethyl benzoyl phosphate(LAP), 40mg hyaluronic acid methacrylate (HAMA), 3mg CuZn MOF MXene composite and 2ml water. Figure 28- depicts the contact lens prepared with the above mentioned formulation.

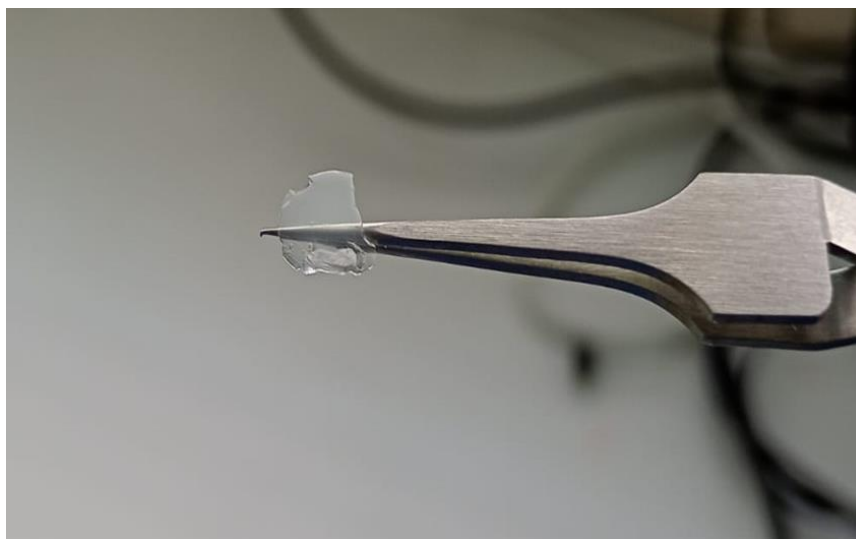


*Figure 28- picture of prepared contact lens*

## 10. Discussion and conclusion

This research main focus was developing a CuZn MOF MXene composite in which metallic ions, in this case  $\text{Cu}^+$  and  $\text{Zn}^+$ , merged with distinctive and exceptional 2D MXene layers. The highly porous MOF was prepared with dimethylimidazole, fabricating a hydrophobic nature MOF due to presence of methyl groups. This hydrophobic property was helpful in the application of this composite for antibacterial coating. The prepared CuZn MOF MXene composite was marked successful after positive results from considerable characterization techniques, XRD, FTIR, SEM and TEM. This composite was highly suitable for bactericidal actions by inhibiting almost 98%

microbial colonies. The soft contact lens was also constructed with HAMA and LAP. There were also some unexpected negative results in which this composite was unable to impede the bacterial colony. The first reason of this issue can be the derogation of MXene as the initial MXene used was almost 6-8 months old. By the time MXene loses its metallic conductivity and surface charge also changes resulting in minimal bacteria killing. There are chances that MXene can lose its properties because of oxidation over period of time if not properly stored and handled.

## 11. Future aspects

This composite manifested promising antibacterial application in the field of ocular diseases. Nonetheless, there is still significant aspects left to enhance this work. Synthesis of this composite can be improved further by diverting the conditions such as pH levels and temperatures. Biocompatibility assessment is essential to be examined due to its application in contact lens and for long-term exposure effects. Cytotoxicity experiments to examine the effect of this composite on human corneal cells. Other drugs along with CuZn MOF MXene composite can also be co-loaded for synergistic effects. This composite can also be applied as a wound dressings with addition of hydrogel. The manufacturing can also be tuned towards green synthesis and 3D printing to make it environmental friendly and also customized the contact lenses according to customer's demand. In vivo studies are also one important factor to inspect the affinity with the real ocular pathogens. Moreover, UV protection, drug releasing period, reusability and transparency are also considerable factors to achieve top-notch CuZn MOF MXene composite based contact lens.

1. Lv R, Robinson JA, Schaak RE, Sun D, Sun Y, Mallouk TE, et al. Transition Metal Dichalcogenides and Beyond: Synthesis, Properties, and Applications of Single- and Few-Layer Nanosheets. *Acc Chem Res.* 2015 Jan 20;48(1):56–64.
2. Progress and Prospects in Transition-Metal Dichalcogenide Research Beyond 2D | Chemical Reviews [Internet]. [cited 2025 May 26]. Available from: <https://pubs-acsc-org.ezproxy.utu.fi/doi/full/10.1021/acs.chemrev.0c00505>
3. Lin X, Li Z, Qiu J, Wang Q, Wang J, Zhang H, et al. Fascinating MXene nanomaterials: emerging opportunities in the biomedical field. *Biomater Sci.* 2021 Aug 10;9(16):5437–71.
4. Saxena A, Tyagi A, Vats S, Gupta I, Gupta A, Kaur R, et al. MXene-Integrated Composites for Biomedical Applications: Synthesis, Cancer Diagnosis, and Emerging Frontiers. *Small Science.* 2025;5(4):2400492.
5. Jiang X, Kuklin AV, Baev A, Ge Y, Ågren H, Zhang H, et al. Two-dimensional MXenes: From morphological to optical, electric, and magnetic properties and applications. *Physics Reports.* 2020 Mar 15;848:1–58.
6. Firouzjaei M, Karimiziarani M, Hamid M, Elliott M, Anasori B. MXenes: The two-dimensional influencers. *Materials Today Advances.* 2022 Mar 1;13:100202.

7. Anasori B, Lukatskaya MR, Gogotsi Y. 2D metal carbides and nitrides (MXenes) for energy storage. *Nat Rev Mater*. 2017 Jan 17;2(2):1–17.
8. Kvashina TS, Uvarov NF, Korchagin MA, Krutskiy YuL, Ukhina AV. Synthesis of MXene Ti<sub>3</sub>C<sub>2</sub> by selective etching of MAX-phase Ti<sub>3</sub>AlC<sub>2</sub>. *Materials Today: Proceedings*. 2020 Jan 1;31:592–4.
9. Gonzalez-Julian J. Processing of MAX phases: From synthesis to applications. *Journal of the American Ceramic Society*. 2021;104(2):659–90.
10. Khazaei M, Arai M, Sasaki T, Estili M, Sakka Y. Trends in electronic structures and structural properties of MAX phases: A first-principles study on M<sub>2</sub>AlC (M = Sc, Ti, Cr, Zr, Nb, Mo, Hf, or Ta), M<sub>2</sub>AlN, and hypothetical M<sub>2</sub>AlB phases. *Journal of Physics Condensed Matter*. 2014 Nov 24;26:505503.
11. Naguib M, Kurtoglu M, Presser V, Lu J, Niu J, Heon M, et al. Two-Dimensional Nanocrystals Produced by Exfoliation of Ti<sub>3</sub>AlC<sub>2</sub>. *Advanced Materials*. 2011;23(37):4248–53.
12. Ghidui M, Lukatskaya MR, Zhao MQ, Gogotsi Y, Barsoum MW. Conductive two-dimensional titanium carbide ‘clay’ with high volumetric capacitance. *Nature*. 2014 Dec;516(7529):78–81.
13. Wang XM, Kou H, Wang J, Teng R, Du X, Lu X. An octahedral magnetic metal organic frameworks for efficient extraction and enrichment of six pesticides with benzene ring prior to high performance liquid chromatography analysis. *J Porous Mater*. 2020 Aug 1;27(4):1171–7.
14. Alhabeab M, Maleski K, Anasori B, Lelyukh P, Clark L, Sin S, et al. Guidelines for Synthesis and Processing of Two-Dimensional Titanium Carbide (Ti<sub>3</sub>C<sub>2</sub>T<sub>x</sub> MXene). *Chem Mater*. 2017 Sep 26;29(18):7633–44.
15. Ampong DN, Agyekum E, Agyemang FO, Mensah-Darkwa K, Andrews A, Kumar A, et al. MXene: fundamentals to applications in electrochemical energy storage. *Nanoscale Research Letters*. 2023 Feb 1;18(1):1–44.
16. Effect of surface functionalization on the electronic transport properties of Ti<sub>3</sub>C<sub>2</sub> MXene | Request PDF. ResearchGate [Internet]. [cited 2025 May 25]; Available from: [https://www.researchgate.net/publication/283193554\\_Effect\\_of\\_surface\\_functionalization\\_on\\_the\\_electronic\\_transport\\_properties\\_of\\_Ti\\_3\\_C\\_2\\_MXene](https://www.researchgate.net/publication/283193554_Effect_of_surface_functionalization_on_the_electronic_transport_properties_of_Ti_3_C_2_MXene)
17. Ghidui M, Halim J, Kota S, Bish D, Gogotsi Y, Barsoum MW. Ion-Exchange and Cation Solvation Reactions in Ti<sub>3</sub>C<sub>2</sub> MXene. *Chem Mater*. 2016 May 24;28(10):3507–14.
18. Lipton J, Röhr JA, Dang V, Goad A, Maleski K, Lavini F, et al. Scalable, Highly Conductive, and Micropatternable MXene Films for Enhanced Electromagnetic Interference Shielding. *Matter*. 2020 Aug 5;3(2):546–57.
19. Yuan Y, Xu X, Xia J, Zhang F, Wang Z, Liu Q. A hybrid material composed of reduced graphene oxide and porous carbon prepared by carbonization of a zeolitic imidazolate framework (type ZIF-8) for voltammetric determination of chloramphenicol. *Microchim Acta*. 2019 Mar 1;186(3):1–8.
20. Xiao B, Li Y chun, Yu X fang, Cheng J bo. MXenes: Reusable materials for NH<sub>3</sub> sensor or capturer by controlling the charge injection. *Sensors and Actuators B: Chemical*. 2016 Nov 1;235:103–9.

21. Pei Y, Zhang X, Hui Z, Zhou J, Huang X, Sun G, et al. Ti<sub>3</sub>C<sub>2</sub>TX MXene for Sensing Applications: Recent Progress, Design Principles, and Future Perspectives. *ACS Nano*. 2021 Mar 23;15(3):3996–4017.
22. Khatami M, Alvarado M, Kong N, Parikh PJ, Lawley MA. Inpatient discharge planning under uncertainty. *IIE Transactions*. 2022 Apr 1;54(4):332–47.
23. Han X, Huang J, Lin H, Wang Z, Li P, Chen Y. 2D Ultrathin MXene-Based Drug-Delivery Nanoplatfom for Synergistic Photothermal Ablation and Chemotherapy of Cancer. *Advanced Healthcare Materials*. 2018;7(9):1701394.
24. Li R, Zhang L, Shi L, Wang P. MXene Ti<sub>3</sub>C<sub>2</sub>: An Effective 2D Light-to-Heat Conversion Material. *ACS Nano*. 2017 Apr 25;11(4):3752–9.
25. Ihsanullah I. Potential of MXenes in Water Desalination: Current Status and Perspectives. *Nano-Micro Lett*. 2020 Mar 12;12(1):72.
26. Qiao Q, Wang J, Li B, Guo Y, Liao T, Xu Z, et al. Ti<sub>3</sub>C<sub>2</sub>Tx MXene nanosheet-based drug delivery/cascaded enzyme system for combination cancer therapy and anti-inflammation. *Applied Materials Today*. 2024 Jun 1;38:102215.
27. Safaei M, Foroughi MM, Ebrahimipoor N, Jahani S, Omidi A, Khatami M. A review on metal-organic frameworks: Synthesis and applications. *TrAC Trends in Analytical Chemistry*. 2019 Sep 1;118:401–25.
28. Introduction to Metal–Organic Frameworks. *Chem Rev*. 2012 Feb 8;112(2):673–4.
29. Shen M, Forghani F, Kong X, Liu D, Ye X, Chen S, et al. Antibacterial applications of metal–organic frameworks and their composites. *Comprehensive Reviews in Food Science and Food Safety*. 2020;19(4):1397–419.
30. Rubio-Martinez M, Avci-Camur C, Thornton AW, Imaz I, Maspoch D, Hill MR. New synthetic routes towards MOF production at scale. *Chem Soc Rev*. 2017 Jun 6;46(11):3453–80.
31. Stock N, Biswas S. Synthesis of Metal-Organic Frameworks (MOFs): Routes to Various MOF Topologies, Morphologies, and Composites. *Chem Rev*. 2012 Feb 8;112(2):933–69.
32. Friščić T. New opportunities for materials synthesis using mechanochemistry. *J Mater Chem*. 2010 Aug 31;20(36):7599–605.
33. Horcajada P, Serre C, Vallet-Regí M, Sebban M, Taulelle F, Férey G. Metal–Organic Frameworks as Efficient Materials for Drug Delivery. *Angewandte Chemie International Edition*. 2006;45(36):5974–8.
34. Mao K, Pruski M. Directly and indirectly detected through-bond heteronuclear correlation solid-state NMR spectroscopy under fast MAS. *Journal of Magnetic Resonance*. 2009 Dec 1;201(2):165–74.
35. Xu J, Terskikh VV, Huang Y. <sup>25</sup>Mg Solid-State NMR: A Sensitive Probe of Adsorbing Guest Molecules on a Metal Center in Metal–Organic Framework CPO-27-Mg. *J Phys Chem Lett*. 2013 Jan 3;4(1):7–11.

36. Gu C, Weng W, Lu C, Tan P, Jiang Y, Zhang Q, et al. Decorating MXene with tiny ZIF-8 nanoparticles: An effective approach to construct composites for water pollutant removal. *Chinese Journal of Chemical Engineering*. 2022 Feb 1;42:42–8.
37. Yao S, Wang Y, Chi J, Yu Y, Zhao Y, Luo Y, et al. Porous MOF Microneedle Array Patch with Photothermal Responsive Nitric Oxide Delivery for Wound Healing. *Advanced Science*. 2022;9(3):2103449.
38. Wittmann T, Siegel R, Reimer N, Milius W, Stock N, Senker J. Enhancing the Water Stability of Al-MIL-101-NH<sub>2</sub> via Postsynthetic Modification. *Chemistry – A European Journal*. 2015 Jan 2;21(1):314–23.
39. Khandelwal G, Maria Joseph Raj NP, Kim SJ. Zeolitic Imidazole Framework: Metal–Organic Framework Subfamily Members for Triboelectric Nanogenerators. *Advanced Functional Materials*. 2020;30(12):1910162.
40. Ma Z, Yuan T, Fan Y, Wang L, Duan Z, Du W, et al. A benzene vapor sensor based on a metal-organic framework-modified quartz crystal microbalance. *Sensors and Actuators B: Chemical*. 2020 May 15;311:127365.
41. Zhu M, Wu X, Niu B, Guo H, Zhang Y. Fluorescence sensing of 2,4,6-trinitrophenol based on hierarchical IRMOF-3 nanosheets fabricated through a simple one-pot reaction. *Applied Organometallic Chemistry*. 2018;32(5):e4333.
42. Tong P, Liang Junyu, Jiang Xinxin, and Li J. Research Progress on Metal–Organic Framework Composites in Chemical Sensors. *Critical Reviews in Analytical Chemistry*. 2020 Jul 3;50(4):376–92.
43. Zhang J, Sun L, Chen C, Liu M, Dong W, Guo W, et al. High performance humidity sensor based on metal organic framework MIL-101(Cr) nanoparticles. *Journal of Alloys and Compounds*. 2017 Feb 25;695:520–5.
44. Yanai N, Kitayama K, Hijikata Y, Sato H, Matsuda R, Kubota Y, et al. Gas detection by structural variations of fluorescent guest molecules in a flexible porous coordination polymer. *Nature Mater*. 2011 Oct;10(10):787–93.
45. Contact Lens Wearer Demographics and Risk Behaviors for Contact Lens-Related Eye Infections – United States, 2014 [Internet]. [cited 2025 May 25]. Available from: <https://www.cdc.gov/mmwr/preview/mmwrhtml/mm6432a2.htm>
46. Cheng KH, Leung SL, Hoekman HW, Beekhuis WH, Mulder PGH, Geerards AJM, et al. Incidence of contact-lens-associated microbial keratitis and its related morbidity. *Lancet*. 1999 Jul 17;354(9174):181–5.
47. Fagan XJ, Jhanji V, Constantinou M, Amirul Islam FM, Taylor HR, Vajpayee RB. First contact diagnosis and management of contact lens-related complications. *Int Ophthalmol*. 2012 Aug 1;32(4):321–7.
48. Mordmuang A, Udomwech L, Karnjana K. Influence of Contact Lens Materials and Cleaning Procedures on Bacterial Adhesion and Biofilm Formation. *Clin Ophthalmol*. 2021;15:2391–402.

49. Willcox MDP. Characterization of the normal microbiota of the ocular surface. *Experimental Eye Research*. 2013 Dec 1;117:99–105.
50. Kaper JB, Nataro JP, Mobley HLT. Pathogenic *Escherichia coli*. *Nat Rev Microbiol*. 2004 Feb;2(2):123–40.
51. Ranjith K, Arunasri K, Reddy GS, Adicherla H, Sharma S, Shivaji S. Global gene expression in *Escherichia coli*, isolated from the diseased ocular surface of the human eye with a potential to form biofilm. *Gut Pathogens*. 2017 Apr 3;9:15.
52. Jones L, Hui A. Release of ciprofloxacin and dexamethasone from commercial contact lens materials. *Contact Lens and Anterior Eye*. 2013 Dec 1;36:e38.
53. Phan CM, Bajgrowicz-Cieslak M, Subbaraman LN, Jones L. Release of Moxifloxacin from Contact Lenses Using an In Vitro Eye Model: Impact of Artificial Tear Fluid Composition and Mechanical Rubbing. *Transl Vis Sci Technol*. 2016 Nov;5(6):3.
54. Manicam C, Perumal N, Wasielica-Poslednik J, Ngongkole YC, Tschäbunin A, Sievers M, et al. Proteomics Unravels the Regulatory Mechanisms in Human Tears Following Acute Renouncement of Contact Lens Use: A Comparison between Hard and Soft Lenses. *Sci Rep*. 2018 Aug 1;8(1):11526.
55. Scribd [Internet]. [cited 2025 May 25]. Contact Lens Practice 3rd | PDF | Contact Lens | Optometry. Available from: <https://www.scribd.com/document/580510252/Contact-Lens-Practice-3rd>
56. Tran NPD, Yang MC, Tran-Nguyen PL. Evaluation of silicone hydrogel contact lenses based on poly(dimethylsiloxane) dialkanol and hydrophilic polymers. *Colloids and Surfaces B: Biointerfaces*. 2021 Oct 1;206:111957.
57. Abdulamier AA, Shaker LM, Al-Amiery AA, Qasim MT, Isahak WNRW, Luthfi AAI. Advancements and applications of smart contact lenses: A comprehensive review. *Results in Engineering*. 2024 Dec 1;24:103268.
58. Revolutionizing contact lens manufacturing: exploring cutting-edge techniques and innovations for enhanced vision and comfort | *International Journal of Low-Carbon Technologies* | Oxford Academic [Internet]. [cited 2025 May 25]. Available from: <https://academic.oup.com/ijlct/article/doi/10.1093/ijlct/ctad136/7616736?login=false>
59. Lin X, Liu J, Zhou F, Ou Y, Rong J, Zhao J. Poly(2-hydroxyethyl methacrylate-co-quaternary ammonium salt chitosan) hydrogel: A potential contact lens material with tear protein deposition resistance and antimicrobial activity. *Biomaterials Advances*. 2022 May 1;136:212787.
60. Tashakori-Sabzevar F, Mohajeri SA. Development of ocular drug delivery systems using molecularly imprinted soft contact lenses. *Drug Development & Industrial Pharmacy*. 2015 May 1;41(5):703–13.
61. Choi SW, Kim J. Therapeutic Contact Lenses with Polymeric Vehicles for Ocular Drug Delivery: A Review. 2018 Jul [cited 2025 May 25]; Available from: <https://www.proquest.com/docview/2131650873?pq-origsite=primo&sourcetype=Scholarly%20Journals>

62. Xu J, Xue Y, Hu G, Lin T, Gou J, Yin T, et al. A comprehensive review on contact lens for ophthalmic drug delivery. *Journal of Controlled Release*. 2018 Jul 10;281:97–118.
63. Ciolino JB, Stefanescu CF, Ross AE, Salvador-Culla B, Cortez P, Ford EM, et al. *In vivo* performance of a drug-eluting contact lens to treat glaucoma for a month. *Biomaterials*. 2014 Jan 1;35(1):432–9.
64. Lv C, Leng J, Qian M, Sun B, Ye H, Li M, et al. Antimicrobial resistance in *Escherichia coli* and *Staphylococcus aureus* at human-animal interfaces on Chongming Island, Shanghai: A One Health perspective. *One Health*. 2024 Oct 5;19:100910.
65. Sanseverino I, Loos R, Navarro Cuenca A, Marinov D, Lettieri T. State of the art on the contribution of water to antimicrobial resistance [Internet]. Publications Office of the European Union; 2018 [cited 2025 May 27]. Available from: <https://data.europa.eu/doi/10.2760/771124>
66. Shah SN, Bhat MA, Bhat MA, Jan AT. Antimicrobial Resistance: An Overview. In: *Nanotechnology Based Strategies for Combating Antimicrobial Resistance* [Internet]. Springer, Singapore; 2024 [cited 2025 May 27]. p. 1–44. Available from: [https://link.springer.com/chapter/10.1007/978-981-97-2023-1\\_1](https://link.springer.com/chapter/10.1007/978-981-97-2023-1_1)
67. Bartholomew JW, Mittwer T. THE GRAM STAIN. *Bacteriol Rev*. 1952 Mar;16(1):1–29.
68. Al-Shalah LAM, Hadi BH, Abood FM, K. Hindi NK, Hamza SA, Jasim AN, et al. Antibacterial Effect of Aqueous Extract of *Theobroma Cacao* Against Gram-Negative and Gram-Positive Bacteria: An in Vitro Study. *Journal of Medicinal and Chemical Sciences*. 2023 Mar 1;6(3):464–71.
69. ResearchGate [Internet]. [cited 2025 May 27]. (PDF) ANTIBACTERIAL PROPERTIES OF *EPILOBIUM* AND OTHER PLANT SPECIES: A SYSTEMATIC REVIEW OF THE LITERATURE. Available from: [https://www.researchgate.net/publication/340061932\\_ANTIBACTERIAL\\_PROPERTIES\\_OF\\_EPILOBIUM\\_AND\\_OTHER\\_PLANT\\_SPECIES\\_A\\_SYSTEMATIC\\_REVIEW\\_OF\\_THE\\_LITERATURE](https://www.researchgate.net/publication/340061932_ANTIBACTERIAL_PROPERTIES_OF_EPILOBIUM_AND_OTHER_PLANT_SPECIES_A_SYSTEMATIC_REVIEW_OF_THE_LITERATURE)
70. Gyawali R, Ibrahim SA. Natural products as antimicrobial agents. *Food Control*. 2014 Dec 1;46:412–29.
71. Reddy M, Kasimsetty S, Jacob M, Khan S, Ferreira D. Antioxidant, Antimalarial and Antimicrobial Activities of Tannin-Rich Fractions, Ellagitannins and Phenolic Acids from *Punica granatum* L. *Planta medica*. 2007 Jun 1;73:461–7.
72. Mandalari G, Bisignano C, D'Arrigo M, Ginestra G, Arena A, Tomaino A, et al. Antimicrobial potential of polyphenols extracted from almond skins. *Letters in Applied Microbiology*. 2010 Jul 1;51(1):83–9.
73. Burt SA, Reinders RD. Antibacterial activity of selected plant essential oils against *Escherichia coli* O157:H7. *Letters in Applied Microbiology*. 2003 Mar 1;36(3):162–7.
74. Wiśniewski P, Trymers M, Chajęcka-Wierzchowska W, Tkacz K, Zadernowska A, Modzelewska-Kapituła M. Antimicrobial Resistance in the Context of Animal Production and Meat Products in Poland—A Critical Review and Future Perspective. *Pathogens*. 2024 Dec;13(12):1123.

75. Shin SY, Bajpai VK, Kim HR, Kang SC. Antibacterial activity of bioconverted eicosapentaenoic (EPA) and docosahexaenoic acid (DHA) against foodborne pathogenic bacteria. *International Journal of Food Microbiology*. 2007 Jan 25;113(2):233–6.
76. Tiwari BK, Valdramidis VP, O’ Donnell CP, Muthukumarappan K, Bourke P, Cullen PJ. Application of Natural Antimicrobials for Food Preservation. *J Agric Food Chem*. 2009 Jul 22;57(14):5987–6000.
77. Okaiyeto S, Xiao HW, Mujumdar A, Sutar P, Ni J. Antibiotic Resistant Bacteria in Food Systems: Current Status, Resistance Mechanisms, and Mitigation Strategies. *Agriculture Communications*. 2024 Feb 3;2.
78. Yang S, Li J, Aweya JJ, Yuan Z, Weng W, Zhang Y, et al. Antimicrobial mechanism of *Larimichthys crocea* whey acidic protein-derived peptide (LCWAP) against *Staphylococcus aureus* and its application in milk. *International Journal of Food Microbiology*. 2020 Dec 16;335:108891.
79. Del Nobile MA, Lucera A, Costa C, Conte A. Food applications of natural antimicrobial compounds. *Front Microbiol* [Internet]. 2012 Aug 8 [cited 2025 May 23];3. Available from: <https://www.frontiersin.org/journals/microbiology/articles/10.3389/fmicb.2012.00287/full>
80. Belfiore C, Castellano P, Vignolo G. Reduction of *Escherichia coli* population following treatment with bacteriocins from lactic acid bacteria and chelators. *Food Microbiol*. 2007 May;24(3):223–9.
81. Mutlu Z, Shams Es-haghi S, Cakmak M. Recent Trends in Advanced Contact Lenses. *Advanced Healthcare Materials*. 2019;8(10):1801390.
82. O’Sullivan L, Ross RP, Hill C. Potential of bacteriocin-producing lactic acid bacteria for improvements in food safety and quality. *Biochimie*. 2002 May 1;84(5):593–604.
83. Reinoso JJ, Enríquez E, Fuertes V, Liu S, Menéndez J, Fernández JF. The challenge of antimicrobial glazed ceramic surfaces. *Ceramics International*. 2022 Mar 15;48(6):7393–404.
84. A AJ, S A, K B, Mv J. Review on the Antimicrobial Properties of Carbon Nanostructures. *Materials (Basel, Switzerland)* [Internet]. 2017 Sep 11 [cited 2025 May 25];10(9). Available from: <https://pubmed.ncbi.nlm.nih.gov/28892011/>
85. Rai M, Yadav A, Gade A. Silver nanoparticles as a new generation of antimicrobials. *Biotechnology Advances*. 2009 Jan 1;27(1):76–83.
86. Vincent M, Hartemann P, Engels-Deutsch M. Antimicrobial applications of copper. *International Journal of Hygiene and Environmental Health*. 2016 Oct 1;219(7, Part A):585–91.
87. Gu H, Ho PL, Tong E, Wang L, Xu B. Presenting Vancomycin on Nanoparticles to Enhance Antimicrobial Activities. *Nano Lett*. 2003 Sep 1;3(9):1261–3.
88. Dash M, Chiellini F, Ottenbrite RM, Chiellini E. Chitosan—A versatile semi-synthetic polymer in biomedical applications. *Progress in Polymer Science*. 2011 Aug 1;36(8):981–1014.
89. Kenawy ER, Worley SD, Broughton R. The chemistry and applications of antimicrobial polymers: a state-of-the-art review. *Biomacromolecules*. 2007 May;8(5):1359–84.

90. Tiller JC, Liao CJ, Lewis K, Klibanov AM. Designing surfaces that kill bacteria on contact. *Proceedings of the National Academy of Sciences*. 2001 May 22;98(11):5981–5.
91. Md. Nordin NAH, Ismail A, Misdan N, Nazri N. Modified ZIF-8 mixed matrix membrane for CO<sub>2</sub>/CH<sub>4</sub> separation. In 2017. p. 020091.
92. Huang Y, Xie Y, Zhao J, Yin X, Chai C. Variety of ZIF-8/MXene-Based Lightweight Microwave-Absorbing Materials: Preparation and Performances of ZnO/MXene Nanocomposites. *J Phys Chem C*. 2022 Aug 18;126(32):13847–53.
93. Li Y, Zhou X, Wang J, Deng Q, Li M, Du S, et al. Facile preparation of in situ coated Ti<sub>3</sub>C<sub>2</sub>T<sub>x</sub>/Ni<sub>0.5</sub>Zn<sub>0.5</sub>Fe<sub>2</sub>O<sub>4</sub> composites and their electromagnetic performance. *RSC Adv*. 2017 May 5;7(40):24698–708.
94. Li Y, Kamdem P, Jin XJ. A Freeze-and-Thaw-Assisted Approach to Fabricate MXene/ZIF-8 Composites for High-Performance Supercapacitors and Methylene Blue Adsorption. *J Electrochem Soc*. 2020 Jul;167(11):110562.